AD_____

Award Number: DAMD17-03-1-0755

TITLE: Therapy of Ovarian Carcinoma by Targeted Delivery of
Alpha-Particles Using Immunoliposomes Capable of
Retaining Alpha-Emitting Daughters

PRINCIPAL INVESTIGATOR: George Sgouros, Ph.D.

CONTRACTING ORGANIZATION: Johns Hopkins University School of
Medicine
Baltimore, Maryland 21205

REPORT DATE: October 2004

TYPE OF REPORT: Annual

PREPARED FOR: U.S. Army Medical Research and Materiel Command
Fort Detrick, Maryland 21702-5012

DISTRIBUTION STATEMENT: Approved for Public Release;
Distribution Unlimited

The views, opinions and/or findings contained in this report are
those of the author(s) and should not be construed as an official
Department of the Army position, policy or decision unless so
designated by other documentation.

20050407 138

REPORT DOCUMENTATION PAGE

Form Approved
OMB No. 074-0188

1. AGENCY USE ONLY (Leave blank)	2. REPORT DATE October 2004	3. REPORT TYPE AND DATES COVERED Annual (30 Sep 2003 - 29 Sep 2004)

4. TITLE AND SUBTITLE
Therapy of Ovarian Carcinoma by Targeted Delivery of Alpha-Particles Using Immunoliposomes Capable of Retaining Alpha-Emitting Daughters

5. FUNDING NUMBERS
DAMD17-03-1-0755

6. AUTHOR(S)
George Sgouros, Ph.D.

7. PERFORMING ORGANIZATION NAME(S) AND ADDRESS(ES)
Johns Hopkins University School of Medicine
Baltimore, Maryland 21205

E-Mail: gsgouros@jhmi.edu

8. PERFORMING ORGANIZATION REPORT NUMBER

9. SPONSORING / MONITORING AGENCY NAME(S) AND ADDRESS(ES)
U.S. Army Medical Research and Materiel Command
Fort Detrick, Maryland 21702-5012

10. SPONSORING / MONITORING AGENCY REPORT NUMBER

11. SUPPLEMENTARY NOTES

12a. DISTRIBUTION / AVAILABILITY STATEMENT
Approved for Public Release; Distribution Unlimited

12b. DISTRIBUTION CODE

13. ABSTRACT (Maximum 200 Words)
The objective of this work is to develop a liposomal system for encapsulating alphaparticle emitting radionuclides for use in IP-administered targeted therapy of ovarian cancer metastases. The scope of the overall project includes development, stability, and radionuclide retention testing of the liposomes as well as the evaluation of their targeting properties, *in vitro*, and *in vivo* (aims 1 and 2). This is to be followed by evaluation of tumor cell kill using monolayer cell culture, spheroid culture and in tumorbearing animals (aims 3 and 4). Substantial progress has been made towards achieving aims 1 and 2. Stable liposomes of different sizes and charge were prepared. Actinium-225 retention was more than 88 % over 30 days. Liposomes were successfully conjugated to trastuzumab, an anti-HER2/neu antibody. A 53-fold increase in HER2/neu+ cell binding was observed for the radioimmunoliposomes compared to non-targeted liposomes. 56% of the cell-associated radioimmunoliposomes were internalized. Studies, *in vivo*, yielded 21.3±19.5%ID/g tumor uptake at 4 hrs post-injection (PI); liver (3.9-24.9%ID/g) and spleen (130.6-296.3%ID/g) accumulation of liposomes was observed at 8 hrs PI. Fluorescent liposomes were detected in intact form in the peritoneal cavity 6 hrs after administration. Efficacy evaluations will be performed in the next 2 years.

14. SUBJECT TERMS
Radioimmunotherapy, alpha-particle, immunoliposome, HER2/neu, Ac-225

15. NUMBER OF PAGES
74

16. PRICE CODE

17. SECURITY CLASSIFICATION OF REPORT Unclassified	18. SECURITY CLASSIFICATION OF THIS PAGE Unclassified	19. SECURITY CLASSIFICATION OF ABSTRACT Unclassified	20. LIMITATION OF ABSTRACT Unlimited

NSN 7540-01-280-5500

Standard Form 298 (Rev. 2-89)
Prescribed by ANSI Std. Z39-18
298-102

Table of Contents

George Sgouros, Ph.D.

Annual Report - Therapy of Ovarian Carcinoma by Targeted Delivery of Alpha-Particles Using Immunoliposomes Capable of Retaining Alpha-Emitting Daughters

INTRODUCTION

Disseminated, metastatic ovarian carcinoma is largely incurable. This project is intended to develop and evaluate targeted, alpha-particle emitter loaded liposomes –alpha radioimmunoliposomes (ARILs)- for therapy of IP-disseminated ovarian cancer metastases. Through previous DOD funding we examined the feasibility of liposomal encapsulation of the potent alpha-particle emitter actinium-225 in order to retain daughter emissions at the targeted site. In this grant we proposed to coat the liposomes with anti-HER2/neu antibodies, test their stability and tumor targeting characteristics, *in vitro* and *in vivo*. The tumor cell killing potential of ARILs as well as their normal organ toxicity will also be evaluated by a combination of studies performed, *in vitro* and *in vivo*.

BODY

The tasks of the proposal and accomplishments in the first year of the grant are outlined below.

Task 1. **Develop 700 to 800 nm-diameter immunoliposomes and characterize their stability and targeting properties, *in vitro* and, *in vivo*.**

Only the results will be summarized, detailed methodology is included in a paper that has been submitted for publication and that is included in the Appendix.

Lipid suspensions were taken through twenty-one cycles of extrusion (LiposoFast, Avestin, Ontario, Canada) through two stacked polycarbonate filters (800 nm filter pore diameter), and unentrapped contents were removed by size exclusion chromatography (SEC). The measured average liposome sizes for the zwitterionic composition was 646 ± 288 nm (diameter) on the day of preparation and 657 ± 365 nm after 30 days. For the cationic composition the corresponding values were 602 ± 385 nm and 678 ± 357 nm, respectively.
To evaluate the stability of liposomes over time, in terms of content retention, calcein (a self-quenching fluorophore) was entrapped into liposomes at high concentrations. Release of calcein, due to membrane instability, results in dilution of the fluorophore by the surrounding solvent, relief of self-quenching, and increase of the fluorescence intensity. The fractional fluorescence self-quenching decrease, $\Delta q \times 100$, is shown on tables 1 and 2 for zwitterionic and cationic liposomes over the period of 30 days at 37°C in media (with 1-10% serum) and in ascites fluid, respectively. Incubation of liposomes in media resulted, after the first 24 hours, in a maximum of 17% decrease in self-quenching, which possibly could be attributed to differences in osmolarity between the encapsulated calcein solution and the liposome surrounding solvent. Beyond this point liposomes were generally stable for over 30 days (Table 1). In ascites fluid, after 15 days of incubation, a 21% decrease in self-quenching was measured for zwitterionic liposomes, and no decrease was observed for cationic liposomes. After incubation for 30

3

days in ascites fluid, more than 50% decrease in self-quenching was observed for both zwitterionic and cationic liposomes.

Table 1

Time [days]	Large Zwitterionic Liposomes $\Delta q \times 100$*			Large Cationic Liposomes $\Delta q \times 100$*		
	1% serum	5% serum	10% serum	1% serum	5% serum	10% serum
1	0±9	0±7	0±6	0±7	0±7	0±6
2	17±9	14±6	6±6	2±6	-2±6	2±5
3	21±8	14±6	8±7	15±7	10±7	15±7
14	22±10	6±6	0±6	32±6	6±6	5±6
30	21±9	-1±6	-9±6	39±6	0±7	-5±6

Table 2

Time [days]	Zwitterionic Liposomes $\Delta q \times 100$*	Cationic Liposomes
1	0±9	0±12
2	0±9	-9±10
3	0±8	-4±11
10	19±8	1±10
15	21±7	0±9
20	47±7	26±9
30	69±7	52±9

* Fractional fluorescence self-quenching decrease due to calcein leakage from PEGylated liposomes over time ($\Delta q_{day\_x} = (q_{day\_1} - q_{day\_x}) / q_{day\_1}$).

Retention of ^{111}In by liposomes

To enable imaging and evaluate retention, the radiometal ^{111}In, was encapsulated into large liposomes. The efficiency of ^{111}In entrapment in liposomes was 5-10% and 73-81% with the passive and chemical loading method, respectively.

The decay-corrected ^{111}In activity that was retained in the zwitterionic and cationic liposomes three days after preparation was >88% and > 87% of the liposome initial activity (on the day of preparation) for the liposomes that were loaded with the passive and chemical method, respectively.

Liposome immunolabelling

The conjugation reaction resulted in 65-90 antibodies per zwitterionic liposome and 90-145 antibodies per cationic liposome. To determine the possible leakage of entrapped contents during conjugation, calcein was encapsulated into liposomes at self-quenching concentrations. No significant change in self-quenching efficiency was detected (data not shown).

Cell binding and internalization of liposomes

To determine binding of liposomes to SKOV3 cells, the liposomal membrane was labeled with a fluorescent phospholipid (rhodamine-PE, 1 mole % of total lipid), and cell suspensions were incubated with immunolabeled and plain liposomes. Also, in parallel measurements for the determination of the specific binding of immunoliposomes to the HER2/neu antigen receptor, SKOV3 cells were previously blocked with excess trastuzumab, the antibody that was also conjugated to immunoliposomes. Figures 1A and 1B show the flow cytometry histograms for binding of zwitterionic immunoliposomes and plain liposomes to SKOV3 cells, respectively, with (shaded gray) and without blocking (thick solid line) of the HER2/neu antigen receptor on the cell surface. A significant shift in fluorescence counts of SKOV3 cells was detected only in the case of immunoliposomes, and only when the HER2/neu receptors on the cell surface were not blocked (Figure 1A, thick solid line). Non-specific binding of plain zwitterionic liposomes to SKOV3 cells was not detected as is depicted by the unchanged fluorescence of cells in Figure 1B. Contrary to zwitterionic liposomes, cationic liposomes exhibit non-specific binding (Figure 1C: shaded gray, and Figure 1D: shaded gray and thick solid line). Binding of cationic immunoliposomes to unblocked SKOV3 cells showed the largest shift in cell fluorescence counts (Figure 1C: thick solid line).

SKOV3 cells were also incubated with TRIC-labeled antibodies. Trastuzumab® (shaded black) but not Rituximab® (an irrelevant antiCD20 antibody, shaded gray) binds specifically to SKOV3 cells, as is shown in Figure 1E.
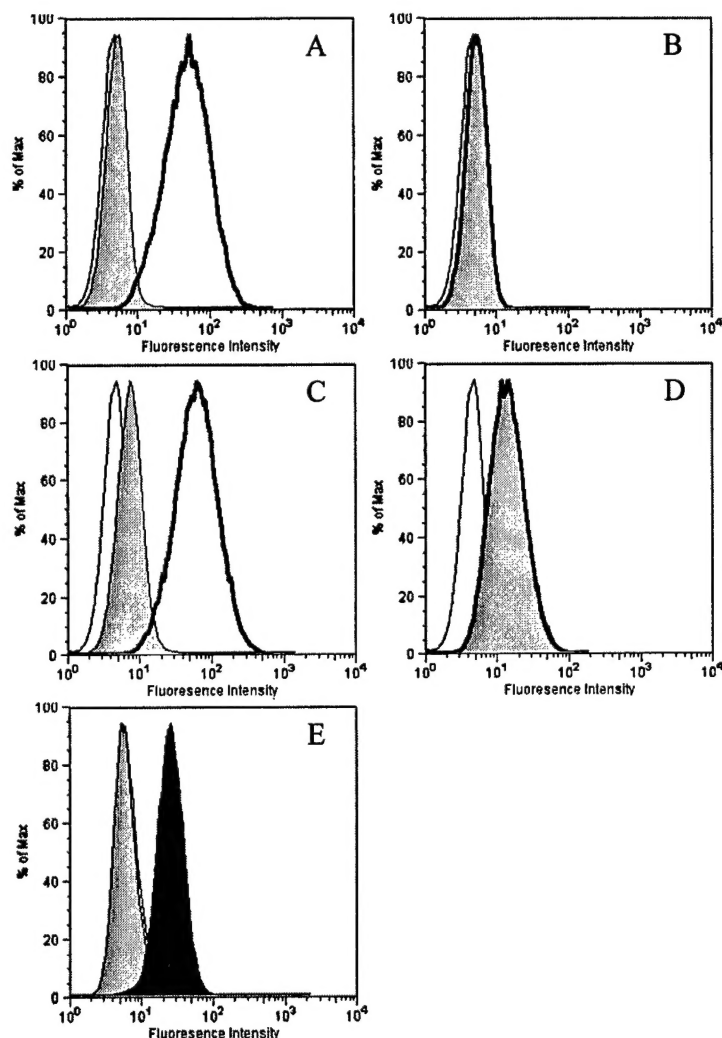

Figure 1. Binding of rhodamine-labeled plain liposomes and immunoliposomes to SKOV3 cells. Thin solid line: SKOV3 cells; Shaded gray: fluorescence of liposomes bound to SKOV3 cells with blocked HER2/neu antigen receptors; Thick solid line: fluorescence of liposomes bound to unblocked SKOV3 cells. (A) Zwitterionic immunoliposomes, (B) Zwitterionic plain liposomes, (C) Cationic immunoliposomes, (D) Cationic plain liposomes, (E) Control. Shaded gray: Binding of TRITC-labeled Rituximab to SKOV3 cells (irrelevant antibody). Shaded black: Binding of TRIC-labeled trastuzumab to SKOV3 cells (relevant antibody).

To quantitatively determine liposomal binding and internalization, liposomes with entrapped ^{111}In were incubated at 37°C with SKOV3 cell suspensions for 0, 0.5, 1, 2, 4 and 24 hours. The total cell-associated radioactivity increased over time of incubation reaching at 4 hours a 4-fold increase for zwitterionic immunoliposomes (Figure 2A) and a 29-fold increase for cationic immunoliposomes (Figure 2B) compared to the values for total cell-associated radioactivity of immunoliposomes at t=0. For zwitterionic immunoliposomes, internalized radioactivity increased 13-fold within the first 4 hours and then remained constant for up to 24 hours (24 hr. time-point not shown on plot). However, the total cell associated intensity continued to rise reaching a 6-fold increase after 24 hours. In other words, internalization and replacement on the cell membrane of the HER2/neu target receptor occurred only the first few hours of incubation. At later times, internalization of the receptor was diminished.

For cationic immunoliposomes, both the total cell-associated radioactivity and the internalized radioactivity increased over 24 hours of incubation (24 hour time point not shown on the plot). No saturation of receptor internalization was observed. At 24 hours, a 189-fold increase in cell-associated radioactivity was observed with a 111-fold increase in internalized counts. The increase in membrane bound activity implies that the HER2/neu target receptor was being replaced on the cell membrane after receptor internalization.

At 24 hours, 1.2% of the total zwitterionic and 13.3% of the total cationic immunoliposome activity was cell-associated. Non-targeted plain liposomes showed low, non-specific, cell-binding (Figures 2A and 2B). Only 0.3% of total zwitterionic and 0.9% of total cationic non-targeted liposome activity was cell-associated.
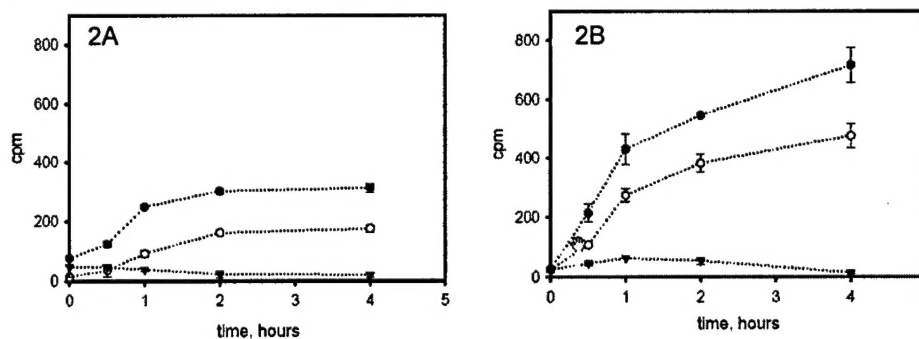

Figure 2. Cell binding and internalization of liposomes. ^{111}In-labeled liposomes were added to ice cold, blocked SKOV3 cells, 10^6cells/ml. Cells were transferred to a 37°C incubator and were sampled at 0, 0.5, 1, 2, 4, and 24 hours. Samples were washed and surface bound liposomes were removed by an acidic stripping buffer at room temperature. The activities of supernatants and pellets were then quantified in a gamma-counter. (A) zwitterionic liposomes, (B) cationic liposomes. ● total cell-associated activity of immunoliposomes, ○ cell internalized activity of immunoliposomes, ▼ total cell-associated activity of plain liposomes. The error bars correspond to standard deviations.

Biodistributions of large liposomes in tumor free mice

The biodistributions and pharmacokinetics of large zwitterionic and cationic plain liposomes, with entrapped ^{111}In-DTPA, were determined, initially, in Balb/c mice without tumor. At 1, 4, 8, and 24 hours post IP administration of liposomal suspensions, animals were killed and the radioactivity distribution of excised tissues was obtained by γ counting. The biodistributions of large zwitterionic and cationic plain liposomes in mice without tumor are shown in Figures 3A and 3B respectively. The most significant normal organ accumulation was in the liver and spleen. 4 hours post-injection of zwitterionic liposomes (Figure 3A) , 3.2 ± 1.3% ID/g and 68.8 ± 40.1% ID/g was accumulated in the liver and spleen, respectively, and at 8 hours the corresponding values were 3.9 ± 3.5% ID/g and 130.6 ± 197.9% ID/g. Cationic liposomes had higher uptake by the liver (Figure 3B). At 4 and 8 hours post-injection 11.2 ± 7.7% ID/g and 24.9 ± 4.5% ID/g of

cationic liposomes was accumulated in the liver. The maximum uptake in the liver and spleen was observed 8 hours post-injection for both liposomal compositions.

The whole body clearance was slow when liposomes were administered. On the contrary, rapid whole body clearance was observed after administration of ^{111}In-DTPA (Figure 3C). Blood uptake and elimination kinetics of zwitterionic liposomes was described by a bi-exponential curve with mean half-lives of 0.51 ± 0.29 hours and 5.79 ± 0.24 hours, respectively. The corresponding values for cationic liposomes were 0.68 ± 0.84 hours and 2.74 ± 0.71 hours. At early time (1-4 hours), blood showed a significant uptake of 6-8% ID/g that may reflect a fraction of rapidly disrupted liposomes after intraperitoneal injection, or smaller size liposomes that escape the peritoneal cavity through lymphatic drainage.
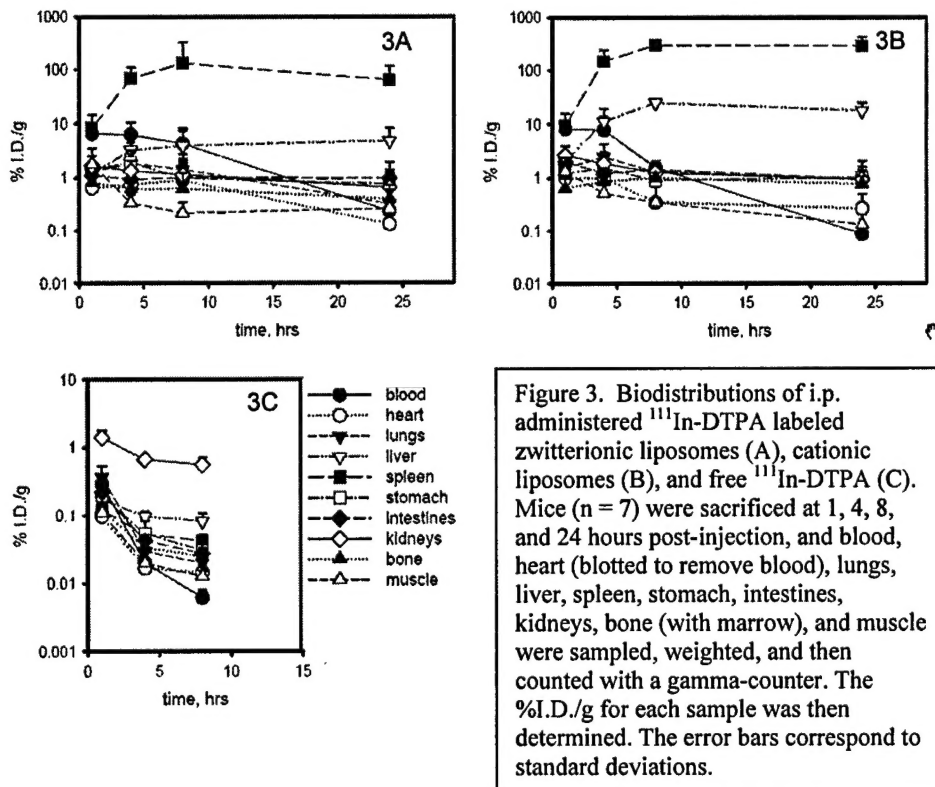

Figure 3. Biodistributions of i.p. administered ^{111}In-DTPA labeled zwitterionic liposomes (A), cationic liposomes (B), and free ^{111}In-DTPA (C). Mice (n = 7) were sacrificed at 1, 4, 8, and 24 hours post-injection, and blood, heart (blotted to remove blood), lungs, liver, spleen, stomach, intestines, kidneys, bone (with marrow), and muscle were sampled, weighted, and then counted with a gamma-counter. The %I.D./g for each sample was then determined. The error bars correspond to standard deviations.

Biodistributions of large zwitterionic liposomes in tumor bearing mice

Biodistributions of plain- and immuno- liposomes were determined in tumor bearing mice. Fourteen days after inoculation, a tumor pattern was formed, that consisted of nodules on the ventral side of the spleen. Smaller nodules (~ 1mm in diameter) were frequently observed within the mesentery. At 14 days post-innoculation, the mean weight of observed tumor nodules was 0.269 ± 0.242 g (n=30, total number of animals).

Four hours after IP administration of large zwitterionic liposomes the tumor uptake of immunoliposomes was $17.6 \pm 3.7\%$ ID/g, and $2.7 \pm 0.7\%$ ID/g for plain non-targeted liposomes (Figures 4A and 4B). Twenty-four hours after administration, the difference in tumor uptake between the two liposomal groups was smaller: $12.0 \pm 4.0\%$ ID/g for immunoliposomes and $8.7 \pm 6.1\%$ ID/g for plain zwitterionic liposomes. The normal

7

organ with the highest uptake was the spleen with $83.3 \pm 19.7\%$ ID/g for zwitterionic immunoliposomes. For non-targeted liposomes the spleen uptake at 4 hours was $33.9 \pm 29.4\%$ ID/g, and at 24 hours it reached the value of $82.5 \pm 49.1\%$ ID/g. Liver had the second highest normal organ uptake. 4 hours after administration, $9.1 \pm 0.4\%$ ID/g of immunoliposomes and $5.0 \pm 1.7\%$ ID/g of plain zwitterionic liposomes were observed in the liver. After 24 hours, the liver uptake increased to $14.1 \pm 2.2\%$ ID/g and $11.1 \pm 2.3\%$ ID/g for immunoliposomes and plain non-targeted liposomes, respectively. Kidney uptake was insignificant. Biodistributions of plain zwitterionic liposomes in mice with and without tumor had no significantly different uptake by the spleen and liver.
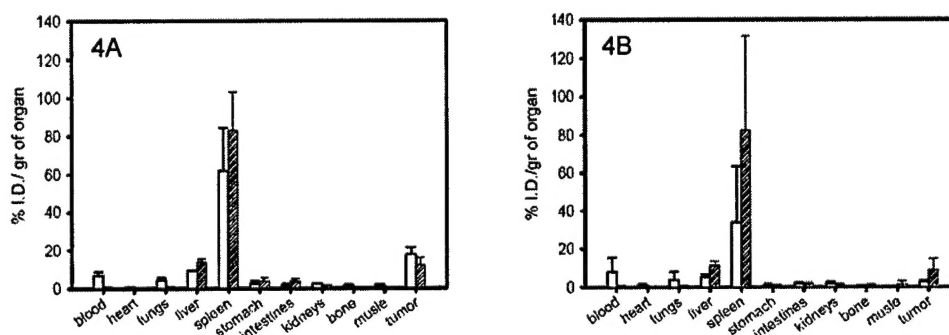

Figure 4. Biodistributions of IP administered ^{111}In-DTPA labeled zwitterionic liposomes. Female athymic nude mice bearing 14-day-old IP xenographs of SKOV3 cells were sacrificed at 4 (open bars) and 24 (shaded bars) hours after administration of immunoliposomes (A) or plain liposomes (B) (n = 3-5), and blood, heart, lungs, liver, spleen, stomach, intestines, kidneys, bone, muscle, and tumor were sampled, weighted, and then counted with a gamma-counter. The %I.D./g for each sample was then determined. The error bars correspond to standard deviations.

Biodistributions of large cationic liposomes in tumor bearing mice
Large cationic liposomes demonstrated a tumor uptake pattern similar to zwitterionic liposomes (Figures 5A and 5B). Four hours after IP administration, tumor uptake was $21.3 \pm 19.5\%$ID/g for cationic immunoliposomes, and $7.1 \pm 2.5\%$ ID/g for plain cationic liposomes; 24 hours after administration, the difference in tumor localization between immunoliposomes ($21.7 \pm 14.3\%$ ID/g) and plain liposomes ($18.6 \pm 12.9\%$ ID/g) was not significantly smaller as observed for zwitterionic liposomes. Spleen uptake increased with time and 24 hours post-injection it reached the value of $148.7 \pm 67.2\%$ ID/g and $161.5 \pm 104.0\%$ ID/g for cationic immunoliposomes and non-targeted liposomes, respectively. Liver uptake, 4 hours post-injection, was $12.9 \pm 11.3\%$ ID/g for immunoliposomes and $10.0 \pm 6.5\%$ ID/g for plain non-targeted liposomes. 24 hours later, it further increased to $21.4 \pm 7.8\%$ ID/g and $16.9 \pm 7.2\%$ ID/g for cationic imunoliposomes and plain liposomes, respectively. Kidney uptake was not significant. Blood uptake was low.
The biodistributions of plain cationic liposomes were similar in tumor bearing and tumor free mice, except for the spleen uptake that was significantly higher in the latter.
Blood uptake for all types of liposomes was between 2.7-8.0% ID/g at 4 hours and dropped to below 0.8% ID/g at 24 hours. Liver and spleen uptake of the cationic radioimmunoliposomes was greater than the corresponding values for zwitterionic

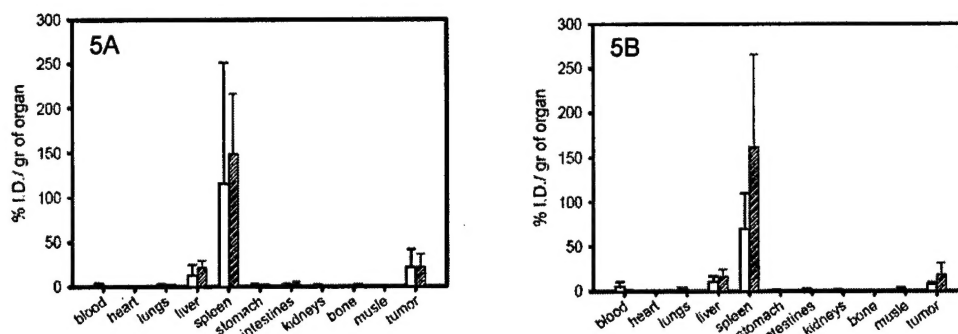immunoliposomes. Both immuno-liposomal compositions showed similar tumor uptake 4 hours after administration.

Figure 5. Biodistributions of IP administered ^{111}In-DTPA labeled cationic liposomes. Female athymic nude mice bearing 14-day-old IP xenographs of SKOV3 cells were sacrificed at 4 (open bars) and 24 (shaded bars) hours after administration of immunoliposomes (A) or plain liposomes (B) (n = 4), and blood, heart, lungs, liver, spleen, stomach, intestines, kidneys, bone, muscle, and tumor were sampled, weighted, and then counted with a gamma-counter. The %I.D./gr for each sample was then determined. The error bars correspond to standard deviations.

Imaging of liposomes in vivo

The distribution of ^{111}In-DTPA entrapping liposomes in mice after IP administration was imaged using a planar gamma-camera (Figure 6). No radioactivity into the circulation was observed, as is shown by the absence of radiation intensity in the cardiac region. The images suggest that liposomes are retained intact in the peritoneal region, since the native distribution of free ^{111}In-DTPA was not observed.
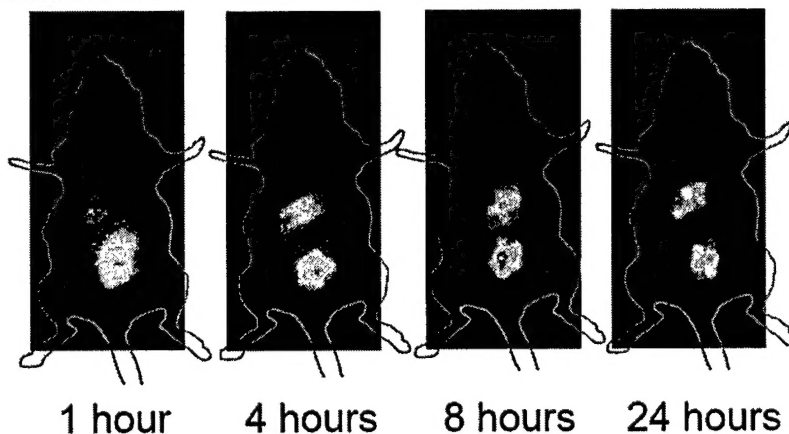

Figure 6. Planar gamma-camera images of mice after IP administration of ^{111}In-DTPA labeled zwitterionic liposomes. Animals were imaged 1, 4, 8, and 24 hours post-injection.

1 hour   4 hours   8 hours   24 hours

Fluorescence imaging of liposomes in the peritoneal cavity

To verify the presence of intact liposomes in the peritoneal cavity at later times after administration, large PEGylated liposomes with an encapsulated fluorophore (calcein), at self-quenching concentrations, were injected intraperitoneally in mice. Six hours later, the animals were sacrificed, the abdominal cavity was exposed and the peritoneal membrane was removed. To detect any intact liposomes in the peritoneal cavity, Triton-X

100 was added to disrupt the intact structures, release calcein from the liposomes, relax self-quenching, and thereby increase the fluorescence intensity. The fluorescence images of the peritoneal cavities of mice are shown in Figures 7A and 7B for animals that were injected with zwitterionic and cationic liposomes, respectively, before the addition of Triton-X 100 (Figures 7A(i) and 7B(i)). After addition of the lipid solubilizer, dramatic increase of fluorescence in the peritoneal fluid was observed for both animals, indicating that 6 hours after IP administration of liposomes, there are still intact liposomes in the peritoneal fluid (Figures 7A(ii) and 7B(ii)).

Mice that were administered fluorescent liposomes were also imaged 48 hours post-injection (data not shown). Intact zwitterionic and cationic liposomes were observed only in the mesentery, as verified by enhancement of the fluorescence intensity after Triton-X 100 addition.
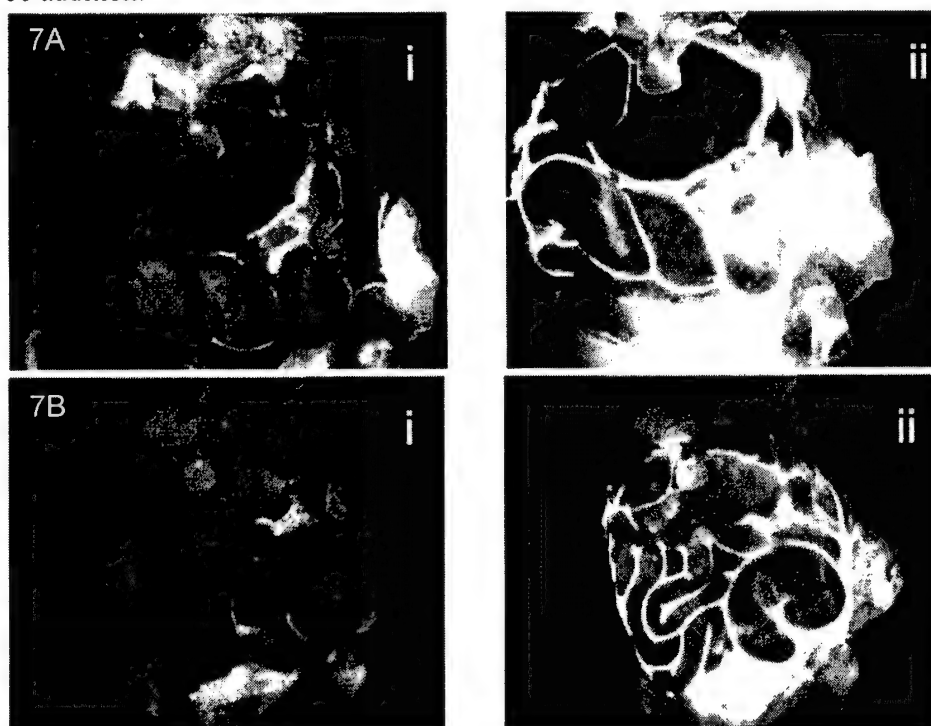

Figure 7. Detection of intact liposomes in the peritoneum using fluorescence imaging of IP administered calcein-containing zwitterionic (A) and cationic (B) liposomes. Mice were sacrificed 6 hours after administration of cationic liposomes with entrapped self-quenching concentrations of calcein. Addition of Triton-X 100 disrupts the intact liposomes, calcein is released from the liposomes, and the fluorescence signal is increased due to relief of self-quenching. (i) Fluorescence image of the peritoneal cavity before addition of Triton-X 100. (ii) After detergent addition.

Task 2. Load the liposomes developed in task 1 with ^{225}Ac and demonstrate >70% daughter retention under various challenge conditions (e.g., 37°C, prolonged serum and high external chelate incubation).

10

The work related to this task has been published and only the abstract is included in this summary. The published paper is included in the Appendix.

Disseminated, metastatic cancer is essentially incurable. Targeted alpha-particle emitters hold great promise as therapeutic agents for disseminated disease. Actinium-225 is a radionuclide generator which has a 10-day half-life and results in alpha-emitting daughter elements (^{221}Fr, ^{217}At, ^{213}Bi) that lead to the emission of a total of four alpha particles. The aim of this study was to develop approaches for stable and controlled targeting of ^{225}Ac to sites of disseminated tumor metastases. Liposomes with encapsulated ^{225}Ac were developed to retain the potentially toxic daughters at the tumor site.

Methods: Actinium-225 was passively entrapped in liposomes. To experimentally test the retention of actinium and its daughters by the liposomes, the gamma emissions of ^{213}Bi were measured in liposome fractions, which were separated from the parent liposome population and the free radionuclides, at different times. Under equilibrium conditions the decay rate of ^{213}Bi was used to determine the concentration of ^{225}Ac. Measurements of the kinetics of ^{213}Bi activity were carried out to estimate the entrapment of ^{213}Bi, the last alpha-emitting daughter in the decay chain.

Results: Stable PEGylated phosphatidylcholine-cholesterol liposomes of different sizes and charge were prepared. Multiple (>2) ^{225}Ac atoms were successfully entrapped per liposome. Actinium-225 retention by zwitterionic liposomes was more than 88 % over 30 days. Retention by cationic liposomes was lower. A theoretical calculation showed that for satisfactory ^{213}Bi retention (>50%), liposomes of relatively large sizes (> 650 nm in diameter) are required. Bismuth-213 retention was experimentally verified to be liposome-size dependent. For large liposomes, the measured ^{213}Bi retention was lower than theoretically predicted.

Conclusions: This work supports the hypothesis that it may be possible to develop ^{225}Ac based therapies by delivering multiple ^{225}Ac atoms in liposomes. Improvements in the retention of ^{225}Ac daughters will likely be necessary to fulfill this potential. Because of the size of the liposomal structures required to contain the daughters, the approach is ideally suited for locoregional therapy (e.g. intraperitoneal, intrahepatic artery, intrathecal).

The low retention of ^{213}Bi has led to the development of a novel liposomal construct – MUVEL for multi-vesicular liposome that is currently being tested. A brief description
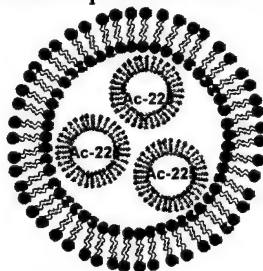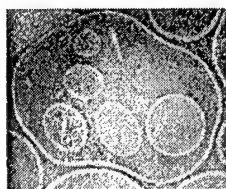
of these is provided below. These constructs are made up of small (100 nm-diameter) unilamelar vesicles within which the ^{225}Ac is encapsulated. These are, in turn, encapsulated into larger (600-700 nm-diameter) liposomes. This approach provides a greater lipid content to which the daughters elements may bind, thereby reducing binding to the inner surface of the larger liposome which would reduce retention of the daughter elements. The figure above, on the left, depicts an electron micrograph showing the structure of the envisioned construct (on the right).

KEY RESEARCH ACCOMPLISHMENTS

- Sterically stabilized, PEGylated and immunolabeled (with Herceptin antibody) liposomes have been generated.
- Their size distribution has been evaluated by dynamic light scattering and electron microscopy.
- Specific targeting and endocytosis of radioimmunoliposomes has been demonstrated, *in vitro*.
- Biodistribution following intraperitoneal injection in tumor-free and tumor-bearing mice using optical imaging and gamma counting, with calcein- and ^{111}In-labeled liposomes, respectively has been evaluated.
- Liposomal loading with ^{225}Ac has been achieved.
- The retention of ^{225}Ac and ^{213}Bi (the last alpha-emitting daughter in the decay chain) have been evaluated.

REPORTABLE OUTCOMES

Sofou S, Thomas JL, Lin H, McDevitt MR, Scheinberg DA, Sgouros G. Engineered liposomes for potential α-particle therapy of metastatic cancer. J Nucl Med 2004; 45:253-260.

Sofou S, Enmon RM., McDevitt MR, Jaggi J, Kappel B, Thomas JL, Scheinberg DA, Sgouros G. Multivesicular radioimmunoliposomes with encapsulated actinium-225 for targeted alpha-particle therapy of intraperitoneal micrometastatic cancer. Presented, orally, at the 10th Conf. on Cancer Therapy with Antibodies & Immunoconjugates, Princeton NJ; 2004.

Sofou S, Enmon RM, Palm S, Kappel B, Zanzonico P, McDevitt MR, Scheinberg DA, Sgouros G. Large radioimmunoliposomes for targeted intraperitoneal therapy of metastatic cancer: binding, internalization and biodistribution studies. Manuscript submitted to J Nucl Med.

Dr. Stavroula Sofou, who was a post-doctoral fellow at the start of this award recently accepted an offer to be Assist Professor in the Dept of Chemical Engineering at the Polytechnic University in NY. The support received from the US Army was instrumental in providing her with the training and experience that made it possible for her to compete for, and obtain this position. She is continuing her focus on breast and ovarian cancer research and has already applied for funding in this area to support her lab and investigate novel targeting structures that have not been previously considered. She will continue to collaborate with the PI for the successful completion of this project. A new post-doc in the PI's lab, Hong Song, has been hired and will continue the work in close collaboration with her.

CONCLUSIONS

We have engineered large antiHER2/neu radioimmunoliposomes that can rapidly and effectively target intraperitoneal tumors in an ovarian carcinoma animal model. Large liposomes are intact in the peritoneal cavity for hours after IP administration, and accumulate to normal organs (liver and spleen) with relatively low rates and at later times. Importantly, no uptake by the kidneys was observed. *In vitro*, large radioimmunoliposomes bind and internalize into SKOV3 cells to a significant extent. Such internalization is favorable as it enables delivery of the radioactivity closer to the nucleus, the target structure for cellular sterilization by radiation.
In the next two years tumor kill and toxicity studies will be performed with large liposomes containing ^{225}Ac and ^{213}Bi. Liposomes loading and retention studies for ^{225}Ac have already been performed and demonstrate adequate long-term retention of the ^{225}Ac but lower retention of the ^{213}Bi than projected from theoretical considerations. We believe that we understand the reasons for this and are developing new constructs to address this problem.

"So What?"

The work performed in the first year of this grant has demonstrated, in preclinical studies, that large radioimmunoliposomes can be used to target metastases of ovarian carcinoma in the peritoneal cavity. Since liposomes clear from the peritoneal cavity much more slowly than antibodies, targeting to cancer cells is improved and the ratio of absorbed dose to tumor cells versus normal organs is likewise improved. This makes it possible to administer greater levels of radioactivity for cancer therapy. In the next two years the efficacy and toxicity of alpha-particle emitter containing radioimmunoliposomes will be evaluated.

REFERENCES

The following references are included in the Appendix.

1. Sofou S, Thomas JL, Lin H, McDevitt MR, Scheinberg DA, Sgouros G. Engineered liposomes for potential α-particle therapy of metastatic cancer. J Nucl Med 2004; 45:253-260.

2. Sofou S, Enmon RM., McDevitt MR, Jaggi J, Kappel B, Thomas JL, Scheinberg DA, Sgouros G. Multivesicular radioimmunoliposomes with encapsulated actinium-225 for targeted alpha-particle therapy of intraperitoneal micrometastatic cancer. Cancer Biother Radiopharm 2004; 19:508-509.

3. Sofou S, Enmon RM, Palm S, Kappel B, Zanzonico P, McDevitt MR, Scheinberg DA, Sgouros G. Large radioimmunoliposomes for targeted intraperitoneal therapy of metastatic cancer: binding, internalization and biodistribution studies. Manuscript submitted to J Nucl Med.

Appendix

1. Sofou S, Thomas JL, Lin H, McDevitt MR, Scheinberg DA, Sgouros G. Engineered liposomes for potential α-particle therapy of metastatic cancer. J Nucl Med 2004; 45:253-260.

2. Sofou S, Enmon RM., McDevitt MR, Jaggi J, Kappel B, Thomas JL, Scheinberg DA, Sgouros G. Multivesicular radioimmunoliposomes with encapsulated actinium-225 for targeted alpha-particle therapy of intraperitoneal micrometastatic cancer. Cancer Biother Radiopharm 2004; 19:508-509.

3. Sofou S, Enmon RM, Palm S, Kappel B, Zanzonico P, McDevitt MR, Scheinberg DA, Sgouros G. Large radioimmunoliposomes for targeted intraperitoneal therapy of metastatic cancer: binding, internalization and biodistribution studies. Manuscript submitted to J Nucl Med.

Engineered Liposomes for Potential α-Particle Therapy of Metastatic Cancer

Stavroula Sofou, PhD[1,2]; James L. Thomas, PhD[3]; Hung-yin Lin, PhD[3]; Michael R. McDevitt, PhD[2]; David A. Scheinberg, MD, PhD[2]; and George Sgouros, PhD[4]

[1]Department of Medical Physics, Memorial Sloan-Kettering Cancer Center, New York, New York; [2]Department of Molecular Pharmacology and Chemistry, Memorial Sloan-Kettering Cancer Center, New York, New York; [3]Department of Chemical Engineering, Columbia University, New York, New York; and [4]Division of Nuclear Medicine, Department of Radiology, Johns Hopkins Medicine, Baltimore, Maryland

Disseminated, metastatic cancer is frequently incurable. Targeted α-particle emitters hold great promise as therapeutic agents for disseminated disease. ^{225}Ac is a radionuclide generator that has a 10-d half-life and results in α-emitting daughter elements (^{221}Fr, ^{217}At, ^{213}Bi) that lead to the emission of a total of 4 α-particles. The aim of this study was to develop approaches for stable and controlled targeting of ^{225}Ac to sites of disseminated tumor metastases. Liposomes with encapsulated ^{225}Ac were developed to retain the potentially toxic daughters at the tumor site. **Methods:** ^{225}Ac was passively entrapped in liposomes. To experimentally test the retention of actinium and its daughters by the liposomes, the γ-emissions of ^{213}Bi were measured in liposome fractions, which were separated from the parent liposome population and the free radionuclides, at different times. Under equilibrium conditions the decay rate of ^{213}Bi was used to determine the concentration of ^{225}Ac. Measurements of the kinetics of ^{213}Bi activity were performed to estimate the entrapment of ^{213}Bi, the last α-emitting daughter in the decay chain. **Results:** Stable pegylated phosphatidylcholine-cholesterol liposomes of different sizes and charge were prepared. Multiple (more than 2) ^{225}Ac atoms were successfully entrapped per liposome. ^{225}Ac retention by zwitterionic liposomes was more than 88% over 30 d. Retention by cationic liposomes was lower. A theoretical calculation showed that for satisfactory ^{213}Bi retention (>50%), liposomes of relatively large sizes (>650 nm in diameter) are required. ^{213}Bi retention was experimentally verified to be liposome-size dependent. For large liposomes, the measured ^{213}Bi retention was lower than theoretically predicted (less than 10%). **Conclusion:** This work supports the hypothesis that it may be possible to develop ^{225}Ac-based therapies by delivering multiple ^{225}Ac atoms in liposomes. Improvements in the retention of ^{225}Ac daughters will likely be necessary to fulfill this potential. Because of the size of the liposomal structures required to contain the daughters, the approach is ideally suited for locoregional therapy (e.g., intraperitoneal, intrahepatic artery, or intrathecal).

Key Words: ^{225}Ac; liposomes; α-particle therapy; ^{225}Ac membrane binding

J Nucl Med 2004; 45:253–260

Disseminated micrometastatic disease is rarely cured by current treatment options. Targeted α-particle emitters hold great promise as therapeutic agents for micrometastases. α-Particles are highly potent cytotoxic agents, potentially capable of tumor-cell kill without limiting morbidity. The increased effectiveness of α-particles is due to the amount of energy deposited per unit distance traveled (linear energy transfer, or LET). For α-particles, this LET is approximately 400 times greater than that of β-particles (80 keV/μm vs. 0.2 keV/μm). Cell survival studies have shown that α-particle–induced killing is independent of oxygenation state or cell-cycle during irradiation and that as few as 1–3 tracks across the nucleus may result in cell death (1–3). In addition, the 50- to 100-μm range of α-particles is consistent with the dimensions of micrometastatic disseminated disease, allowing for localized irradiation of target cells with minimal normal-cell irradiation.

Human use of antibody-targeted α-particle emitters has been reported in 2 trials (4–6). The first injection of an α-particle emitter to humans for radioimmunotherapy was of ^{213}Bi conjugated to the anti-CD33 antibody HuM195, targeting myeloid leukemia (5–7). This trial demonstrated feasibility and anticancer activity with minimal toxicity. In the second of the 2 human trials, the antitenascin antibody 81C6, labeled with the α-particle emitter ^{211}At, was injected into surgically created cavities in patients with malignant gliomas. This trial has demonstrated substantially better tumor control relative to ^{131}I-labeled 81C6 antibody (4). In the setting of minimal disease, animal studies have shown that α-particle emitters yield superior tumor control relative to β-emitters (8–13).

In this study, the α-particle–emitting element generator ^{225}Ac was proposed for potential use in treatment of micrometastatic disease. ^{225}Ac has a 10-d half-life, and its decay, and those of its daughters, lead to the emission of 4 α-particles (Fig. 1).

To deliver an increased number of ^{225}Ac atoms at the target site, liposomes with encapsulated multiple ^{225}Ac atoms were proposed. Liposomes are closed structures de-
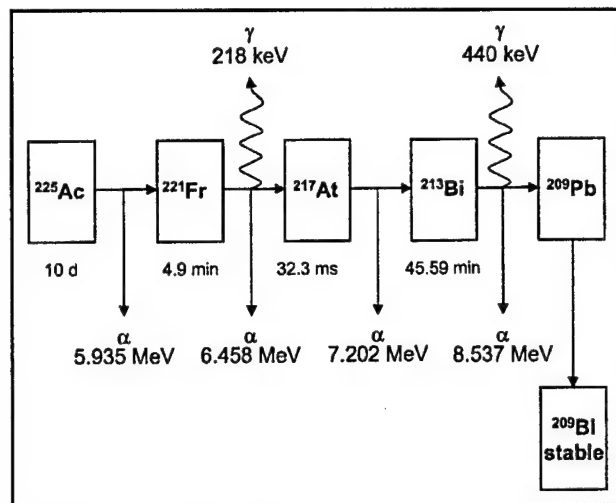
FIGURE 1. Simplified ^{225}Ac decay cascade with associated particulate decays and half-lives.

fined by a phospholipid bilayer membrane that encloses an aqueous compartment (*14*). α-Particles traverse the phospholipid membrane without energy dissipation. Liposomes have been studied for more than 30 y, in particular as vehicles for drug delivery (*15,16*). Their application in drug delivery has been made possible by the development of sterically stabilized structures that use polyethylene glycol (PEG) chains to reduce uptake and catabolism of intravenously administered liposomes by the reticuloendothelial system, thereby increasing circulatory half-life. Such liposomes are typically 100–150 nm in diameter since this size range reduces reticuloendothelial system uptake while retaining adequate aqueous volume for drug delivery. Liposome tumor localization is dependent on the differential permeability of normal- versus tumor-tissue capillaries (*17–19*). Liposomes have also been used to deliver radionuclides, primarily for tumor diagnosis and infectious site imaging (*20,21*).

Studies in animals have shown that ^{225}Ac is substantially more potent and more toxic than ^{213}Bi (*12,22,23*). The toxicity arises because conjugation to antibodies or other molecular vehicles for targeting of this radionuclide can stably deliver only the first of the 4 α-particle–emitting atoms for several reasons: First, the bond between the targeting vehicle and the chelate holding the radionuclide may be broken on transformation of the parent to new daughter and emission of the first α-particle; second, the new daughter has chemistry different from that of the parent; and third, there is recoil of the parent atom away from the chelate. Subsequent α-particle–emitting intermediates (daughters) are, therefore, free to distribute throughout the body and to irradiate healthy organs and tissues.

Liposomes with encapsulated ^{225}Ac should also retain the α-emitting intermediates at the tumor site. Because of their position in the periodic table, the daughters of ^{225}Ac are likely to be ionic (Fr^{+1}, At^{-1}, Bi^{+3}). The hydrophobic region

of liposomal membranes provides a barrier to loss by diffusion of ionic species entrapped in the internal aqueous compartment (*24*). Therefore, if ^{225}Ac is initially entrapped within the aqueous compartment of liposomes, the daughters are expected to be retained within the liposomes. Some loss is unavoidable, however, because the recoil distance traveled by daughter atoms, on decay of the parent, is on the order of the liposome size.

In this study, the feasibility of engineering liposomal vesicles capable of retaining ^{225}Ac and its daughters for cancer therapy was investigated.

MATERIALS AND METHODS

Reagents

The lipids L-α-phosphatidylcholine (egg), 1,2-dipalmitoyl-sn-glycero-3-phosphoethanolamine-*N*-[methoxy(polyethylene glycol)-2000] (ammonium salt) (PEG-labeled lipid), 1,2-dipalmitoyl-sn-glycero-3-ethylphosphocholine (chloride salt), L-α-phosphatidylethanolamine-*N*-(4-nitrobenzo-2-oxa-1,3-diazole) (egg) (NBD-PE), and L-α-phosphatidylethanolamine-*N*-(lissamine rhodamine B sulfonyl) (egg) (purity > 99%) were purchased from Avanti Polar Lipids. Cholesterol, ascorbic acid, phosphate-buffered saline (PBS), fluorexon (calcein), and Sephadex G-50 were purchased from Sigma. 1,4,7,10-Tetraazacyclododecane-1,4,7,10-tetraacetic acid (DOTA) was obtained from Macrocyclics. Dithionite (sodium hydrosulfite, technical grade, approximately 85%) was obtained from Acros Organics. ^{225}Ac was obtained from Oak Ridge National Laboratory.

Liposome Preparation

Mixtures of phosphatidylcholine, cholesterol (1:1 molar ratio) and PEG-labeled lipids (6-mol percentage of total lipid) in CHCl$_3$ were dried in a rotary evaporator. For stability measurements, the lipids were resuspended in calcein solution (55 mmol/L calcein in phosphate buffer, isosmolar to PBS, pH = 7.4). For ^{225}Ac passive entrapment, the lipids were resuspended in PBS containing chelated actinium complexes (^{225}Ac-DOTA, 1.85–3.70 MBq) (*12*) and diethylenetriaminepentaacetic acid. The lipid suspension was then annealed to 55°C for 2 h (*25*). To make liposomes, the lipid suspension was then taken through 21 cycles of extrusion (LiposoFast; Avestin) through 2 stacked polycarbonate filters (100-, 400-, and 800-nm filter pore diameter). Unentrapped contents were removed by size exclusion chromatography (SEC) in a Sephadex G-50 packed 1 × 10 cm column, eluted with an isotonic buffer. Ascorbic acid (8 mmol/L) was coentrapped to minimize lipid oxidation due to radiation (*26*).

To make unilamellar liposomes for radionuclide binding measurements, the above procedure was repeated. The lipids were resuspended in sucrose solution (138 mmol/L, pH = 7.4) isosmotic to PBS and extruded through filters with a 100-nm pore diameter. Unentrapped sucrose was removed by dilution of the liposome suspension in PBS, followed by ultracentrifugation (2 h, 142,000*g*, 25°C). The pellet (10% v/v) was resuspended in PBS and used for the ^{225}Ac binding measurements. The unilamellar character of the zwitterionic and cationic liposomes was tested using dithionite. Dithionite ion S$_2$O$_4^-$ and the spontaneously produced SO$_2^-$ radical react with the NBD-PE–labeled lipids of the outer membrane layer and produce nonfluorescent derivatives (*27*). They diffuse very slowly through the bilayer and thus allow the

quantitative distinction of the inner- and outer-layer lipids. In our NBD-PE–labeled vesicle preparations, unilamellarity was verified by a 51% ± 4% (zwitterionic liposomes) and 55% ± 4% (cationic liposomes) decrease of the initial fluorescence on dithionite addition.

Liposome Stability Measurements

To study the liposome stability (retention of entrapped contents), a fluorescent dye (calcein) was encapsulated at self-quenching concentrations. Different liposome sizes (100-, 400-, and 800-nm filter pore diameter) were examined. The fluorescence intensity of liposome suspensions was measured by a fluorescence microplate reader (excitation wavelength, 485 nm; emission wavelength, 538 nm). Destabilization of the liposomal membrane causes calcein leakage from the liposomes. Calcein leakage is followed by dilution of calcein into the surrounding solution and relief of the fluorescence self-quenching effect, which results in increase of fluorescence intensity. To normalize and properly compare different samples, Triton X-100 (4.5% w/w) was added to the suspension to achieve complete calcein release. To characterize liposome stability, the fluorescence self-quenching efficiency q of liposome suspensions was compared over the period of 30 d (q = I_{max}/I, where I is the measured fluorescence intensity before Triton X-100 addition and I_{max} is the maximum fluorescence intensity after Triton X-100 addition).

Liposome Size Distribution Determination

Dynamic light scattering (DLS) of liposome suspensions was studied with an N4 Plus autocorrelator (Beckman-Coulter), equipped with a 632.8-nm He–Ne laser light source. Scattering was detected at 15.7°, 23.0°, 30.2°, and 62.6°. Particle size distributions at each angle were calculated from autocorrelation data analysis by CONTIN (28). The average liposome size was calculated to be the y-intercept at zero angle of the measured average particle size values versus $sin^2(\theta)$ (29). All buffer solutions used were filtered with 0.22-μm filters just before liposome preparation. The collection times for the autocorrelation data were 1–4 min.

Transmission Electron Microscopy

To observe the size and external morphology of liposomes, a transmission electron microscope (JEOL) was used at 80 kV following the negative staining method. Liposome suspensions were added dropwise to a 400-mesh copper grid coated with polyvinyl formal. After allowance for liposome adhesion, excess sample was removed with filter paper. Staining was obtained with isotonic uranyl acetate solution (2%) in phosphate buffer.

Actinium and Bismuth Retention Measurements

As shown in Figure 1, ^{225}Ac ($t_{1/2} = 10$ d) decays to the following α-emitting radionuclides (respective half-lives shown): ^{221}Fr (4.9 min), ^{217}At (32 msec), and ^{213}Bi (45.6 min). To experimentally test the retention of ^{225}Ac and its daughters by the liposomes, the γ-emissions of ^{221}Fr and ^{213}Bi were measured using a Cobra γ-counter (Packard Instrument Co., Inc.). Under steady-state conditions (after 24 h), the decay rate of each species in the decay chain must be equal; thus, at steady state, the decay rate of either francium or bismuth can be used to determine the actinium concentration. Measurements of the kinetics of ^{213}Bi activity ($t_{1/2}$ is 45.6 min) in liposome fractions separated from the parent liposome population and the unentrapped radionuclides, at different times, allow for estimation of the stability of ^{213}Bi entrapment. In particular, if ^{213}Bi is not leaking, then the ^{213}Bi activity concentration

(measured by γ-counting), after SEC, would be the same over several hours of measurement. If ^{213}Bi is leaking, the ^{213}Bi γ-emissions from the liposome fraction will be low initially, since ^{213}Bi has been lost from the liposomes: Had bismuth been retained, the radioactivity of the vesicle fraction would have been at steady state with ^{225}Ac (i.e., at ~100%). In this newly separated liposome fraction, the bismuth activity rises with monoexponential kinetics (with kinetic constant almost equal to ^{213}Bi half-life) as ongoing actinium decay gradually brings the entire fraction into steady state. Extrapolation of the monoexponential fit curve to the time point of chromatographic separation gives the fractional ^{213}Bi retention by the liposomes. For each liposome population, ^{213}Bi activity was measured after repeated SEC (Sephadex G-50) at various time points. The statistical significance of differences in ^{213}Bi retention for different-sized liposomes was determined by obtaining the area under the retention-versus-time curve for each measurement set. The statistical significance of differences in area under the retention-versus-time curve were then evaluated by a Student (2-tailed) t test (SigmaPlot, SPSS Inc.)

Theoretical Model

To evaluate the theoretical limits of daughter entrapment, a model was developed using nuclear theory and geometry. The nuclear recoil distances of the α-decays of the actinium daughters are not well established in aqueous media, but estimates to within 10%–20% were made (30) using a standard computer model. The range of the recoil distances for francium, astatine, and bismuth were estimated as 81.7, 86.5, and 94.7 nm, respectively. Because these differ by less than the experimental uncertainties, both in the recoil range estimates and in our experimental measurements, a single recoil distance was used to simplify further calculations. With this model, unilamellar liposomes were considered. Each entrapped radionuclide was distributed uniformly within the aqueous volume of a liposome. Thus, each disintegration has a fixed probability f for daughter ejection. The probability of ejection f_{r,r_d} for a disintegration, which occurs at a distance r from the center of a liposome of radius r_l, may then be calculated from geometry (r_d is the recoil distance). The probability f is calculated by averaging the ejection probability f_{r,r_d} over the possible locations of the radionuclide, r:

$$f_{r,r_d} = \begin{cases} 1 - \dfrac{2rr_d - r_l^2 + r^2 + r_d^2}{4rr_d}, & r > r_l - r_d \\ 1, r < r_l - r_d \end{cases}$$

$$f = \int_0^{r_l} 4\pi f_{r,r_d} r^2 dr / \tfrac{4}{3}\pi r_l^3.$$

Retention of bismuth requires 3 successive decays without escape; therefore, the probability is f^3.

Binding Measurements of ^{225}Ac and ^{225}Ac-DOTA to Liposomes

Different activities of ^{225}Ac and ^{225}Ac-DOTA, ranging from 10 Bq to 6 kBq, were mixed in PBS with sucrose-loaded liposomes (2 mmol/L total lipid), and the system was allowed to equilibrate for at least 1 h at room temperature. Rhodamine-labeled zwitterionic and cationic liposomes were present at the same concentrations as those used for the measurement of ^{225}Ac and ^{213}Bi retention by the above liposomes. After ultracentrifugation for 2 h at 142,000g, (25°C), the supernatant (the top 90% of the sample volume) was
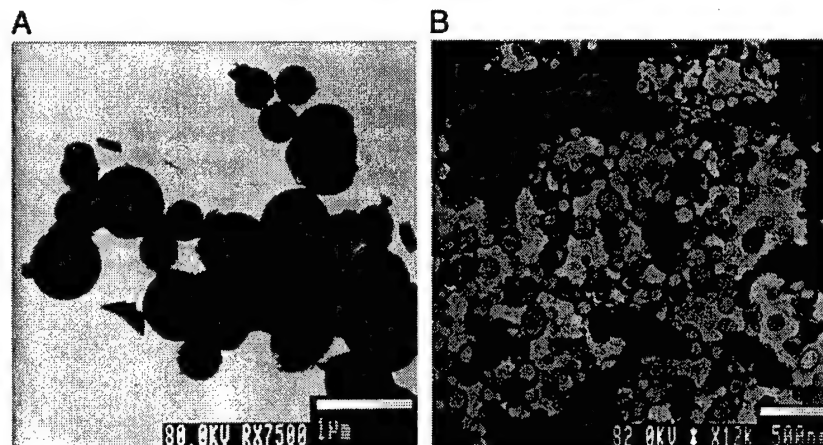
FIGURE 2. Negative-staining transmission electron microscopy images of liposomes prepared with 800-nm (A) and 100-nm (B) filter diameter.

promptly removed. Lipid in both supernatant and pellet was measured using the rhodamine fluorescence intensity (excitation wavelength, 544 nm; emission wavelength, 590 nm). ^{225}Ac activity concentration was measured by the γ-emissions of ^{213}Bi decay at equilibrium. The calculated amount of membrane-bound ^{225}Ac was corrected for the amount of lipid that remained in the supernatant as follows: β, the fraction of bound ^{225}Ac, was defined as the ratio of the bound ^{225}Ac to the total ^{225}Ac in the sample. It was assumed that the concentrations of unbound ^{225}Ac in the pellet $[Ac]_{p,f}$ and in the supernatant were equal, since the distribution of free ^{225}Ac atoms along the tube axis should not be influenced by the separation process. Thus, for the pellet, the average amount of ^{225}Ac bound per lipid (B) would be $B = ([Ac]_{p,t} - [Ac]_{p,f})/[L]_p$, where $[Ac]_{p,t}$ is the total concentration of ^{225}Ac in the pellet and $[L]_p$ is the lipid concentration in the pellet. Because not all the liposomes were found in the pellet, B was used to calculate the bound ^{225}Ac in the supernatant and the true free ^{225}Ac concentration.

RESULTS

Liposome Characterization

Liposomes were prepared by the extrusion method with different filter pore sizes. Liposome size distributions were determined with DLS. The measured average liposome sizes for the zwitterionic composition were 183 ± 83 nm (100-nm filter diameter), 402 ± 185 nm (400-nm filter diameter), and 646 ± 288 nm (800-nm filter diameter). For the cationic composition the corresponding values were 184 ± 74 nm (100-nm filter diameter), 415 ± 153 nm (400-nm filter diameter), and 602 ± 385 nm (800-nm filter diameter). Liposome size distributions were stable during a period of 30 d (data not shown). Liposomes were also imaged by transmission electron microscopy using the negative staining method (Fig. 2).

To evaluate the stability of the liposomal membrane over time, calcein was entrapped into liposomes at high concentration. Release of calcein, because of liposome instability, results in dilution of the fluorophore into the surrounding buffer solution, relief of self-quenching, and an increase in the fluorescence intensity. The fractional fluorescence self-quenching decrease, $\Delta q \times 100$, is shown in Table 1 for zwitterionic and cationic liposomes during the 30 d. Both liposome formulations and all liposome sizes showed a small release of calcein within the first 24 h after preparation; this may have been caused by differences in osmolarity between the encapsulated calcein solution and the liposome surrounding solvent or by membrane defect relaxation. Af-

TABLE 1
Percentage Decrease in Self-Quenching with Time

Time (d)	Zwitterionic liposomes $\Delta q \times 100$*			Cationic liposomes $\Delta q \times 100$*		
	800 nm	400 nm	100 nm	800 nm	400 nm	100 nm
1	0 ± 2	0 ± 2	0 ± 3	0 ± 2	0 ± 2	0 ± 2
2	11 ± 2	14 ± 3	13 ± 3	16 ± 3	20 ± 2	20 ± 3
3	14 ± 2	14 ± 3	3 ± 3	14 ± 3	19 ± 3	17 ± 3
10	18 ± 2	18 ± 2	19 ± 3	17 ± 5	25 ± 2	24 ± 3
20	17 ± 2	16 ± 2	18 ± 3	20 ± 2	24 ± 2	26 ± 2
30	14 ± 3	15 ± 3	19 ± 6	19 ± 4	22 ± 4	27 ± 6

*Fractional fluorescence self-quenching decrease due to calcein leakage from pegylated liposomes over time ($\Delta q_{day\_x} = (q_{day\_1} - q_{day\_x})/q_{day\_1}$). The uncertainties correspond to SEs of repeated measurements.

After first 24 h, a maximum of 20% in self-quenching decrease was measured for all liposomes. Beyond this point, all liposomes were stable for more than 30 days.

ter the second day, and during the 30 d, all types of liposomes were stable. The same behavior was observed for liposomes in media with 1%–10% serum at 37°C (data not shown). The effect of radiation on the stability of liposomes was studied by DLS. The liposome size distributions of samples that contained ^{225}Ac did not change over time.

Retention of ^{225}Ac by Liposomes

As stated in the Materials and Methods, ^{225}Ac retention in liposomes can be determined by the ^{221}Fr or ^{213}Bi activities at steady state. At different time points, liposome fractions were separated from free ^{225}Ac by SEC, and the γ-photons of ^{213}Bi decay at steady-state were used to determine ^{225}Ac retention. Independent of time, the ^{225}Ac activity retained in the zwitterionic liposome fractions was >88% (Fig. 3). ^{225}Ac retention decreased (Fig. 4) over time in the cationic liposomes (cationic lipid: 10-mol percentage of total lipid), but even after 30 d the retention was more than 54%. ^{225}Ac mean encapsulation efficiency in liposomes, using passive entrapment, was 6.4%, with a maximum value of 10.0%.

Theoretical Calculations

The toxicity of ^{225}Ac is in part due to release of its α-particle–emitting daughters. Retention of daughters within the liposomes and at the tumor site would enhance the potential of ^{225}Ac toward α-particle therapy.

The mechanism for daughter loss from the liposome interior is likely to be nuclear recoil. The theoretical fraction of ^{213}Bi retention as a function of liposome size is shown in Figure 5 assuming a recoil distance of 87.6 nm—the average recoil distance in water calculated using the software program Stopping and Range of Ions in Matter, or SRIM. ^{213}Bi is the last α-emitting intermediate on the ^{225}Ac scheme, and thus retention of ^{213}Bi requires retention of both ^{221}Fr and ^{217}At. Adequate ^{213}Bi retention (>50%) requires large liposomes (>650 nm in diameter) (Fig. 5).
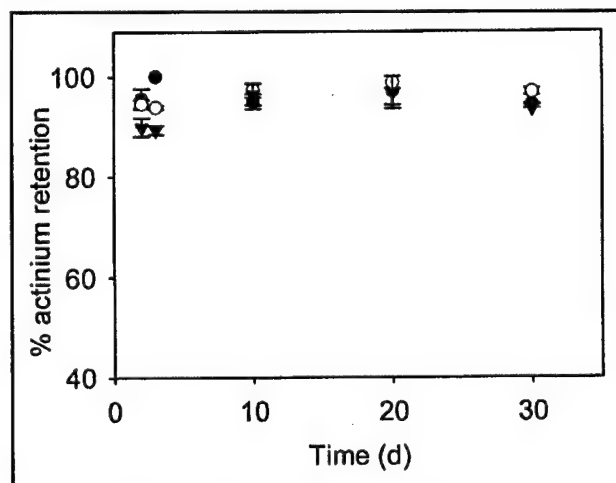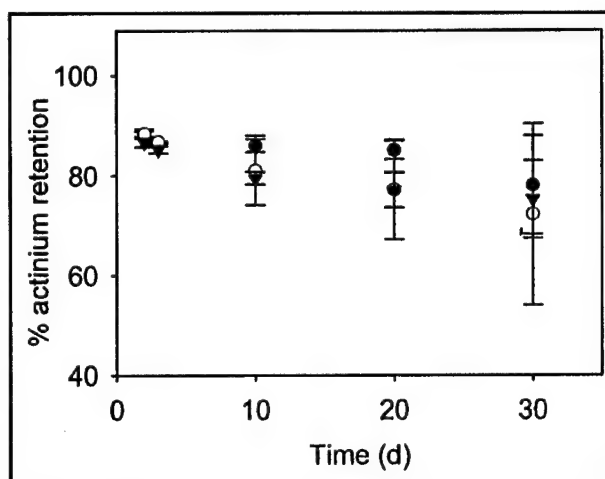

FIGURE 4. Fraction of ^{225}Ac retention by cationic liposomes (filter diameters: 100 (●), 400 (○), and 800 (▼) nm) during 30 d. The error bars correspond to SEs of repeated measurements.

Theoretical retention was also calculated assuming that ^{225}Ac and its daughters localize at the inner liposome membrane; this represents a worst-case scenario. In this case, the maximum ^{213}Bi retention approaches $1/2^3 = 12.5\%$ for large liposomes (8.1% for 650-nm-diameter liposomes). Half the recoils from the surface of an infinitely large vesicle would result in daughter ejection. Thus, if even a fraction of the daughters of ^{225}Ac (or of ^{225}Ac itself) associates with the liposomal membrane, the ^{213}Bi retention will be significantly reduced.

Retention of ^{213}Bi by Liposomes

The retention of ^{213}Bi by liposomes was studied as a function of liposome size and composition. For each lipo-

FIGURE 3. Fraction of ^{225}Ac retention by zwitterionic liposomes (filter diameters: 100 (●), 400 (○), and 800 (▼) nm) during 30 d. The error bars correspond to SEs of repeated measurements.
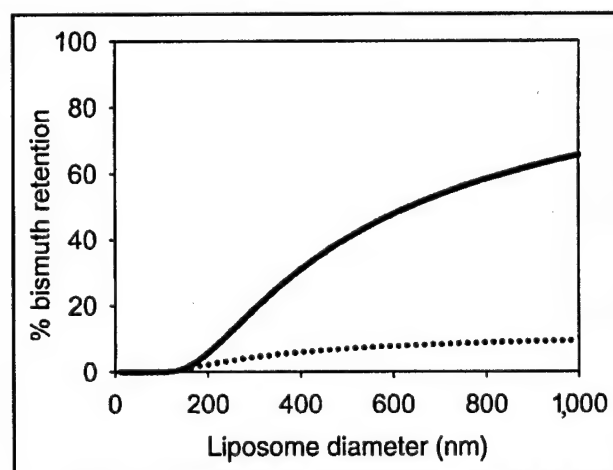

FIGURE 5. Theoretical predictions of ^{213}Bi retention for different liposome sizes (solid line). Radionuclides were assumed to be uniformly entrapped into the liposomal aqueous compartment. The average recoil distance of 87.6 nm was used for all α-emitting intermediates to simplify calculations. Binding of radionuclides to the liposomal membrane will significantly reduce retention (dotted line).
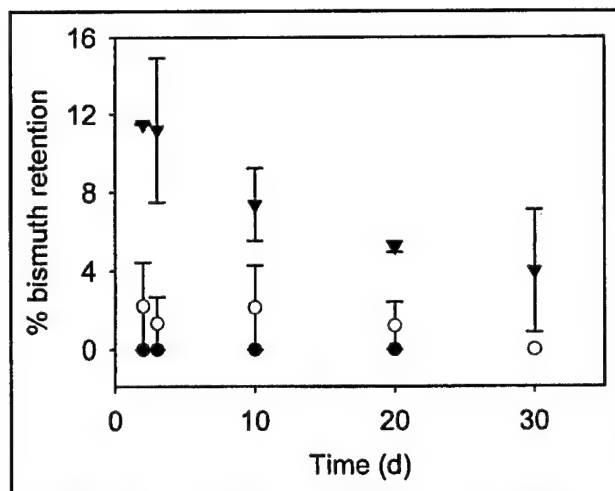
FIGURE 6. Fraction of ^{213}Bi retention by zwitterionic liposomes (filter diameters: 100 (●), 400 (○) and 800 (▼) nm) during 30 d. The error bars correspond to SEs of repeated measurements (for some data points, error bars are smaller than the symbol sizes). For day 30, ^{213}Bi retention for 100- and 400-nm liposomes is 0%, and data points overlap. ^{213}Bi retention in 800-nm liposomes was significantly higher than that in 100-nm liposomes ($P = 0.0044$).

some population, measurements of ^{213}Bi activity were made after repeated chromatography at various time points (Figs. 6 and 7). For large liposomes, retention was much less than theoretically predicted. For both liposome compositions and all sizes examined, the values of ^{213}Bi retention were consistent with the theoretical results for localization of the radionuclides on the liposome membrane.

Binding of ^{225}Ac and ^{225}Ac-DOTA to Liposomal Membranes

Binding of ^{225}Ac and ^{225}Ac-DOTA to zwitterionic and cationic liposomes was measured using an ultracentrifugation assay. In this binding assay, sucrose-loaded liposomes were permitted to bind ^{225}Ac, in free or chelated form, for at least 1 h at room temperature and then were separated by ultracentrifugation. Measurement of ^{225}Ac and lipids was performed on the pellet and supernatant, as described in the Materials and Methods. The liposome concentration was kept constant and equal to that used in the retention experiments, and the radionuclide activity was varied over 4 orders of magnitude, encompassing the activities used in the retention experiments. Significant membrane binding of ^{225}Ac was observed with zwitterionic and cationic liposomes. The number of radionuclide atoms was low compared with the number of binding sites present (concentration of lipid molecules); thus, no saturation on the binding profile was observed. The partition constants K_p ($K_p = C_{bound} C^{-1}_{free} L^{-1}$, C, L [=] mol/L) were expressed as the ratio of bound to free radionuclide atoms, normalized to the concentration of lipid present (L). For the zwitterionic membranes, K_p values were 420 (for ^{225}Ac) and 60 (for ^{225}Ac-DOTA), and for the cationic membranes, 550 and 50, re-

spectively. In our measurements, 30%–35% of ^{225}Ac was bound to membrane under the experimental conditions (accessible lipid L = 1 mmol/L).

DISCUSSION

The ^{225}Ac atomic generator is a promising α-particle–emitting radionuclide for cancer therapy. ^{225}Ac and its α-emitting daughters lead to the emission of a total of 4 α-particles. Loss and widespread dissemination of daughters from the site of parent generator decay will lead to toxicity, whereas confinement to the targeted site will increase efficacy (7,31). This work is part of a study that ultimately aims to target ^{225}Ac to sites of disseminated tumor micrometastases while also retaining the ^{225}Ac α-emitting daughters at the targeted sites. Toward this goal, the use of liposomes is proposed to deliver multiple ^{225}Ac atoms per liposome and to retain the ^{225}Ac progeny in the liposomes and consequently at the targeted sites.

Pegylated liposomes of different membrane charge (zwitterionic and cationic) and size were prepared to entrap ^{225}Ac. They were characterized for content leakage (calcein release) and size (DLS) over time. Liposomes were stable during a period of 30 d. Even in the presence of radiation (from ^{225}Ac), the liposome size distributions were stable over time. Zwitterionic liposomes retained more than 88% of ^{225}Ac for more than 30 d. ^{225}Ac retention in cationic liposomes was lower but still above 54%.

Passive entrapment for ^{225}Ac encapsulation was used in this work. This approach yielded a maximum efficiency of 10% of the initial radioactivity. At initial radioactivity concentrations in the range of 11–37 MBq/mL, this efficiency translates into 10–40 actinium atoms per liposome. Im-
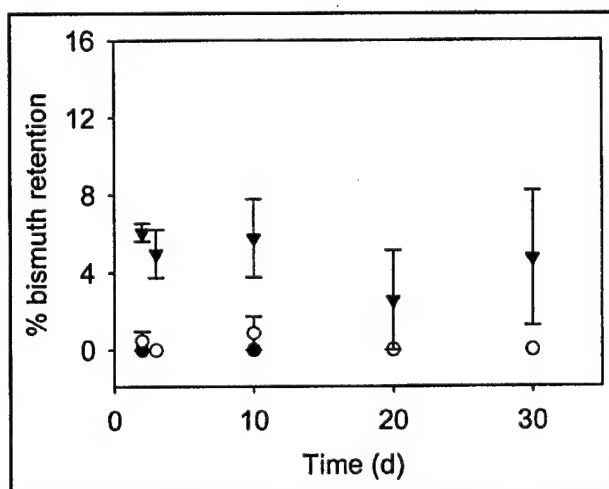

FIGURE 7. Fraction of ^{213}Bi retention by cationic liposomes (filter diameters: 100 (●), 400 (○) and 800 (▼) nm) during 30 d. The error bars correspond to SEs of repeated measurements (for some data points, error bars are smaller than the symbol sizes). For days 20 and 30, ^{213}Bi retention for 100- and 400-nm liposomes is 0%, and data points overlap.

mune-mediated endocytosis of such antibody-coated liposomes would deliver a much larger number of radioactive atoms to a tumor cell than would be possible with radiolabeled antibodies, given currently achievable specific activities.

An important, yet theoretically anticipated, finding of this work is that liposome size is critical in determining daughter retention, implicating nuclear recoil as a critical mechanism for daughter loss in the liposomal encapsulation strategy. Because ^{225}Ac daughters are most probably ionic (Fr^{+1}, At^{-1}, Bi^{+3}), passive permeation (diffusion) through the lipid membrane will be negligible. Based on a geometric model, large, 650-nm-diameter, liposomes are required to yield >50% retention of ^{213}Bi, the last α-emitting daughter in the decay chain. For both liposome compositions and all sizes of liposomes examined, the values of ^{213}Bi retention were consistent with the theoretical results for localization of the radionuclides on the liposome membrane. ^{213}Bi retention was significantly higher in the 800- versus the 100-nm zwitterionic liposomes. No statistically significant difference was seen between 400- and 800-nm zwitterionic liposomes. Likewise, no statistically significant difference in ^{213}Bi retention was seen between the 800- and 100-nm liposomes among the different cationic liposomes. Measurement of the extent of association of Fr^{+1}, At^{-1}, and Bi^{+3} to liposomal membranes is not possible because of their short half-lives compared with the length of the measurement process. Nevertheless, partitioning of the ionic α-emitting intermediates to the liposomal membrane is possible. Binding or association of inorganic monovalent ions to noncharged hydrophilic surfaces, such as phospholipid membranes, has been treated theoretically (32) and verified experimentally (33). In addition, certain anions have the tendency to associate with phosphatidylcholine lipids (32). The partition of Ac^{+3} and Ac^{+3}-DOTA was measured, however, and only a small fraction of the chelated ^{225}Ac partitioned to the liposomal membrane. On the contrary, the measured partitioning of unchelated Ac^{+3} to zwitterionic and cationic membranes was significantly higher. Continuing work focuses on the improvement of ^{213}Bi retention by modification of the membrane affinity.

The theoretical calculations, confirmed by the experimental results, showed that relatively large liposomal sizes are required for adequate daughter retention. (The relatively large liposome sizes required, 650 nm in diameter, are still much smaller than the average cell size, 20 μm. Cells are typically 10,000-fold greater in volume than the largest liposomes considered in this work.) The application of these liposomal systems will focus on locoregional and intracavitary therapy of disseminated micrometastases (34). Liposomes of large size are rapidly cleared from blood circulation (35). Future developments may contribute to better understanding of the clearance mechanism. Targeted delivery can in principle be achieved with appropriate antibodies attached at the terminal end of the PEG chains; this geometry provides exposed antibody molecules that protrude from the liposome for unhindered antigen recognition. Similarly engineered liposomes have been shown to achieve increased cellular uptake by receptor-mediated endocytosis (36).

CONCLUSION

^{225}Ac is a highly potent, but also a potentially highly toxic, α-emitting atomic generator. ^{225}Ac is the parent in a chain of 4 α-particle emitters (^{221}Fr, ^{217}At, ^{213}Bi) and is thus a good candidate radionuclide for cancer therapy. To investigate this approach, multiple ^{225}Ac atoms per liposome were successfully encapsulated within phosphatidylcholine-cholesterol pegylated vesicles and were stably retained for more than 30 d.

Retention of ^{225}Ac radioactive daughters at the tumor site will provide ^{225}Ac with exceptional potential toward α-particle therapy. It was shown that daughter retention depends on liposome size because of daughter nuclear recoil. Measurements of ^{213}Bi retention by liposomes suggested that the α-emitting daughters apparently localize at the liposomal membrane and thus significantly reduce ^{213}Bi retention. Further, improvement of ^{213}Bi retention is being investigated. This work will make it possible to retain the high potency of ^{225}Ac while reducing the toxicity, thereby making it a more feasible approach for cancer therapy.

REFERENCES

1. Humm JL. A microdosimetric model of astatine-211 labeled antibodies for radioimmunotherapy. *Int J Radiat Oncol Biol Phys.* 1987;13:1767–1773.
2. Humm JL, Chin LM. A model of cell inactivation by alpha-particle internal emitters. *Radiat Res.* 1993;134:143–150.
3. Macklis RM, Kinsey BM, Kassis AI, et al. Radioimmunotherapy with alpha-particle-emitting immunoconjugates. *Science.* 1988;240:1024–1026.
4. Zalutsky MR, Cokgor I, Akabani G, et al. Phase I trial of alpha-particle-emitting astatine-211 labeled chimeric anti-tenascin antibody in recurrent malignant glioma patients [abstract]. *Proc Am Assoc Cancer Res.* 2000;41:544.
5. Jurcic JG, McDevitt MR, Sgouros G, et al. Targeted alpha-particle therapy for myeloid leukemias: a phase I trial of bismuth-213-HuM195 (anti-CD33) [abstract]. *Blood.* 1997;90:(suppl 1)504a.
6. Sgouros G, Ballangrud A, Jurcic JG, et al. Pharmacokinetics and dosimetry of an alpha-particle emitter labeled antibody: 213Bi-HuM195 (anti-CD33) in patients with leukemia. *J Nucl Med.* 1999;40:1935–1946.

7. Jurcic JG, Larson SM, Sgouros G, et al. Targeted alpha-particle immunotherapy for myeloid leukemia. *Blood.* 2002;100:1233–1239.

8. Behr TM, Behe M, Stabin MG, et al. High-linear energy transfer (LET) alpha versus low-LET beta emitters in radioimmunotherapy of solid tumors: therapeutic efficacy and dose-limiting toxicity of [213]Bi- versus ^{90}Y-labeled CO17–1A Fab' fragments in a human colonic cancer model. *Cancer Res.* 1999;59:2635–2643.

9. Behr TM, Sgouros G, Stabin MG, et al. Studies on the red marrow dosimetry in radioimmunotherapy: an experimental investigation of factors influencing the radiation-induced myelotoxicity in therapy with beta-, Auger/conversion electron-, or alpha-emitters. *Clin Cancer Res.* 1999;5:3031s–3043s.

10. Kennel SJ, Mirzadeh S. Vascular targeted radioimmunotherapy with [213]Bi: an alpha-particle emitter. *Nucl Med Biol.* 1998;25:241–246.

11. Zalutsky MR, McLendon RE, Garg PK, Archer GE, Schuster JM, Bigner DD. Radioimmunotherapy of neoplastic meningitis in rats using an alpha-particle-emitting immunoconjugate. *Cancer Res.* 1994;54:4719–4725.

12. McDevitt MR, Ma D, Lai LT, et al. Tumor therapy with targeted atomic nanogenerators. *Science.* 2001;294:1537–1540.

13. Zhang M, Zhang Z, Garmestani K, et al. Pretarget radiotherapy with an anti-CD25 antibody-streptavidin fusion protein was effective in therapy of leukemia/lymphoma xenografts. *Proc Natl Acad Sci USA.* 2003;100:1891–1895.

14. Cullis PR, DeKruijff B. Lipid polymorphism and the functional role of lipids in biological membranes. *Biochim Biophys Acta.* 1979;559:399–420.

15. Lasic DD. Novel applications of liposomes. *Trends Biotechnol.* 1998;16:307–321.

16. Drummond DD, Meyer O, Hong K, Kirpotin DB, Papahadjopoulos D. Optimizing liposomes for delivery of chemotherapeutic agents to solid tumors. *Pharmacol Rev.* 1999;51:691–743.

17. Huang SK, Martin FJ, Jay G, Vogel J, Papahadjopoulos D, Friend DS. Extravasation and transcytosis of liposomes in Kaposi's sarcoma-like dermal lesions of transgenic mice bearing the HIV tat gene. *Am J Pathol.* 1993;143:10–14.

18. Wu NZ, Da D, Rudoll TL, Needham D, Whorton AR, Dewhirst MW. Increased microvascular permeability contributes to preferential accumulation of stealth liposomes in tumor tissue. *Cancer Res.* 1993;53:3765–3770.

19. Yuan F, Leunig M, Huang SK, Berk DA, Papahadjopoulos D, Jain RK. Microvascular permeability and interstitial penetration of sterically stabilized (stealth) liposomes in a human tumor xenograft. *Cancer Res.* 1994;54:3352–3356.

20. Boerman OC, Storm G, Oyen WJG. Sterically stabilized liposomes labelled with In-111 to image focal infection in rats. *J Nucl Med.* 1995;36:1639–1644.

21. Emfietzoglou D, Kostarelos K, Sgouros G. An analytic dosimetry study for the use of radionuclide-liposome conjugates in internal radiotherapy. *J Nucl Med.* 2001;42:499–504.

22. Kennel SJ, Brechbiel MW, Milenic DE, Schlom J, Mirzadeh S. Actinium-225 conjugates of MAb CC49 and humanized delta CH2CC49. *Cancer Biother Radiopharm.* 2002;17:219–231.

23. Kennel SJ, Chappell LL, Dadachova K, et al. Evaluation of Ac-225 for vascular targeted radioimmunotherapy of lung tumors. *Cancer Biother Biopharm.* 2000; 15:235–244.

24. Cevc G, Marsh D. *Phospholipid Bilayers: Physical Principles and Models.* New York, NY: Wiley; 1987:190–193.

25. Castile JD, Taylor KMG. Factors affecting the size distribution of liposomes produced by freeze-thaw extrusion. *Int J Pharm.* 1999;188:87–95.

26. Stensrud G, Redford K, Smistad G, Karlsen J. Effects of gamma irradiation on solid and lyophilised phospholipids. *Rad Phys Chem.* 1999;56:611–622.

27. McIntyre JC, Sleight RG. Fluorescence assay for phospholipid membrane asymmetry. *Biochemistry.* 1991;30:11819–11827.

28. Provencher SW. A constrained regularization method for inverting data represented by linear algebraic or integral equations. *Comput Phys Commun.* 1982; 27:213–227.

29. Teraoka I. *Polymer Solutions: An Introduction to Physical Properties.* New York, NY: John Wiley & Sons; 2002:188–191.

30. Ziegler J. *The Stopping and Range of Ions in Matter* [SRIM Web site]. Available at: http://www.srim.org. Accessed Nov. 18, 2003.

31. Sgouros S. Long-lived alpha emitters in radioimmunotherapy: the mischievous progeny. *Cancer Biother Biopharm.* 2000;15:219–221.

32. Cevc G. The molecular mechanism of interaction between monovalent ions and polar surfaces, such as lipid bilayer membranes. *Chem Phys Letters.* 1990;170: 283–288.

33. Binder H, Zschoernig O. The effect of metal cations on the phase behavior and hydration characteristics of phospholipid membranes. *Chem Phys Lipids.* 2002; 115:39–61.

34. Rippe B, Rosengren BI, Venturoli D. The peritoneal microcirculation in peritoneal dialysis. *Microcirculation.* 2001;8:303–320.

35. Ahl PL, Bhatia SK, Meers P, et al. Enhancement of the in vivo circulation lifetime of L-a-distearoylphosphatidylcholine liposomes: importance of liposomal aggregation versus complement opsonization. *Biochim Biophys Acta.* 1997; 1329:370–382.

36. Park JW, Kirpotin DB, Hong K, et al. Tumor targeting using anti-her2 immunoliposomes. *J Control Release.* 2001;74:95–113.

body, a dose that was well below the MTD. The results of the pilot study and additional results from this in progress follow up study will be presented.

15

A MODEL OF METASTATIC BREAST CARCINOMA FOR TARGETED ALPHA-EMITTER THERAPY MODELING/DOSIMETRY STUDIES

H Song, K Shahverdi, J Fox, Y Wang, B Gimi, M Pomper, Z Bhujwalla, RT Reilly, G Sgouros
Johns Hopkins University, School of Medicine, Baltimore, United States

Using a transgenic mouse model of HER2/neu-expressing breast carcinoma, a model for metastatic breast cancer has been developed and characterized for evaluating targeted [213]Bi (alpha-emitter) therapy in the presence of cross-reactive normal organs. HER-2/*neu* transgenic (Neu-N) mice, express the nontransforming rat *neu* cDNA under the mouse mammary tumor virus promoter (MMTV). As a consequence, these mice exhibit high expression of neu in the mammary glands and lower expression in other tissues, including the salivary glands, spleen, thymus, and lungs. Left cardiac ventricle (LCV) injection of 105 neu-expressing NT2 tumor cells, derived from spontaneous mammary tumors in female neu-N mice, yield widespread metastases in the liver and osteolytic metastases in the bone/bone marrow requiring animal sacrifice by $3^1/_2$ to 4 weeks at which time the mice exhibit IP ascites fluid and occasional hind limb paralysis. MicroPET imaging using [^{18}F]fluoride and [^{18}F]FDG has allowed visualization of disease in the bone, bone marrow and liver, *in vivo*. Small animal MR imaging (diffusion-weighted, T1) has revealed a pattern of dissemination in which tumor originating in the bone marrow is seen to lyse cortical bone and invade the surrounding muscle and/or spinal cord regions. To assess response following targeted [213]Bi therapy, the radiosensitivity of the NT2 cell line to [213]Bi alpha-irradiation has been measured by colony formation assay and a D0 of 0.9 Gy was found. The α/β ratio for photon irradiation was 1.0 Gy ($\alpha = 0.0645$ Gy^{-1} $\beta = 0.0662$ Gy^{-2}). The α/β value is consistent with late responding tissue, meaning that fractionation of photon radiation would not be an appropriate strategy for treating tumors derived from this cell line. The alpha-particle cell-survival curve, on the other hand did not exhibit a shoulder, consistent with the well established failure to repair alpha-particle damage. Fractionation of a targeted alpha-emitter in this situation would be highly effective. A relative biological efficacy (RBE) of 3.5, consistent with published studies of other cell lines, was derived from these data. The response of spheroids derived from this cell line to [213]Bi alpha-irradiation was also evaluated. At 1 MBq/ml (27 μCi/ml) [213]Bi using a non-specific antibody with a 24-hour incubation, 12 of 12, 200 μm-diameter spheroids failed to re-grow over a 30-day period; untreated spheroids grew exponentially with a 3 to 4-day doubling time. A nonspecific antibody was used to evaluate inherent radiosensivity of NT2 spheroids, independent of targeting. A mathematical model has been developed to fit doseresponse data obtained from the spheroid and animal models for use in examining feasibility of [213]Bi targeting of rapidly accessible metastases in the presence of cross-reactive normal organs in humans.

16

MULTIVESICULAR RADIOIMMUNOLIPOSOMES WITH ENCAPSULATED ACTINIUM-225 FOR TARGETED ALPHA-PARTICLE THERAPY OF INTRAPERITONEAL MICROMETASTATIC CANCER

S Sofou,[1] RM Enmon,[1] MR McDevitt,[1] J Jaggi,[1] JL Thomas,[2] DA Scheinberg,[1] G Sgouros[3]
[1]Memorial Sloan-Kettering Cancer Center-Program In Molecular Pharmacology And Chemistry, New York, United States
[2]University of New Mexico -Department of Physics And Astronomy, Albuquerque, United States
[3]Johns Hopkins University-Department of Radiology, Baltimore, United States

Targeted alpha-particle emitters hold great promise as therapeutic agents for micrometastatic disease. Because of their high energy deposition, only 1 to 3 alpha-particle traversals through the cell nucleus are required for cell sterilization. In addition, the short range of alpha-particles (50-100 microns) is consistent with the dimensions of micrometastatic disease, allowing for minimal normal cell irradiation. Actinium-225 is an alpha-particle emitter with a 10 day half-life; because actinium decay generates three alpha-particle emitting daughters, it is an attractive candidate for alpha therapy.

Animal studies have demonstrated that [225]Ac-conjugated anti-tumor antibodies are highly potent at sterilizing tumors but that they can also be highly toxic. The high potency arises because tumor-cell bound radiolabeled antibody that internalizes will deliver the alpha-particle emissions arising from all three daughters to the tumor cell since the charged daughters have a low probability of diffusing across the tumor cell membrane. However, the decay of [225]Ac breaks the antibody-conjugate bond thereby assuring delivery of only the first alpha-particle with subsequent alphas delivered at the site of daughter diffusion. Thus, toxicity arises because decay of antibody-conjugated [225]Ac in the vascular or extracellular space will release the daughters into the circulation and potentially lead to normal organ irradiation.

We have investigated encapsulation of [225]Ac in liposomes as a means of retaining daughter alpha-particle emissions at the site of liposomal delivery (Sofou et al., J Nucl Med. 2004 Feb;45(2):253-60). Daughter retention was liposome size dependent, but was lower than expected for the larger liposomes. This was shown to be caused, in part, due to binding of [225]Ac to the phospholipid membrane. Actinium-225 localization to the liposomal membrane increases daughter loss due to nuclear recoil, compared to daughter loss from uniformly distributed [225]Ac atoms within the liposomal aqueous phase.

To increase daughter retention, [225]Ac was passively entrapped in multivesicular liposomes (MUVEL). MUVELs are large liposomes with entrapped smaller vesicles, containing [225]Ac. This strategy provides confinement of entrapped [225]Ac within the region of the liposomal aqueous part, away from the outer liposomal membrane, and also results in decreased radionuclide partition to the external membrane (surface), due to increased internal membrane. MUVELs were prepared and characterized for content leakage and size, over time, and entrapment efficiency. Daughter retention was evaluated by measuring the retention of the last daughter in the decay series ([213]Bi), since escape of prior

intermediates would also lead to [213]Bi loss. MUVELs yielded 98% [225]Ac retention and a daughter retention that led to a 2.6-fold increase in alpha-particle delivery over that expected from [225]Ac alone.

PEGylated MUVELs were then labeled with the anti-HER2/neu monoclonal antibody trastuzumab. Binding of liposomes to ovarian carcinoma cells (SKOV3) was strongly enhanced by immunolabeling. Cellular internalization of immunolabeled liposomes was also considerable. The biodistributions of radioimmunoliposomes in female nude mice bearing intraperitoneal tumors showed significant tumor uptake.

We propose that radioimmunolabeled MUVELs could make it possible to retain the high potency of [225]Ac while reducing the toxicity associated with untargeted daughter emissions thereby enhancing its potential for cancer therapy.

17

ANTITUMOR EFFECT OF AT-211-RADIO-IMMUNOTHERAPY ON SUBCUTANEOUS HUMAN OVARIAN CANCER XENOGRAFTS: EVALUATION OF RBE OF AN ALPHA EMITTER IN VIVO

TA Bäck,[1] S Palm,[1] S Lindegren,[1] B Karlsson,[1]
R Hultborn,[2] L Jacobsson[1]
[1]Dep of Radiation Physics, Göteborg University,
Sahlgrenska University Hospital, Göteborg, Sweden
[2]Dep of Oncology, Göteborg University, Sahlgrenska
University Hospital, Göteborg, Sweden

The use of alpha-particle emitters in radioimmunotherapy appear promising, taking advantage of the short range and the high LET. In a series of preclinical studies we have previously shown convincing results in the treatment of microscopic intraperitoneal ovarian cancer on nude mice, using the alpha emitter At-211. As part of the preparation for our clinical trial with At-211, the current in vivo study on nude mice was carried out to evaluate the RBE of [211]At-MX35 in a RIT model, as compared to external Co-60 gamma irradiation. Our endpoint was growth inhibition on subcutaneous xenografts of the human ovarian cancer cell line NIH:OVCAR-3.

Methods: Growth inhibition following irradiation was studied on subcutaneous xenografts of the human ovarian cancer cell line NIH:OVCAR-3 implanted on nude mice. At different levels of radioactivity administered (0.33, 0.65 and 0.90 MBq) the animals received an injection in the tail vein of [211]At-labeled monoclonal antibody MX35. A control group received unlabeled MX35 only. A separate biodistribution study established uptake of At-211 in tumors and organs at different times after injection. Mean absorbed dose to the tumors were then calculated using the MIRD formalism.

External irradiation of tumor was carried out as a Co-60 whole body irradiation at a low dose rate (2 Gy/h). Using a slide calliper, tumour growth was monitored continuously by volume measurement every second day up to 60 days after treatment. For each individual measurement, a normalized tumour growth (NTG) was calculated by dividing the current tumor volume by its initial volume. An apparent cell survival (ACS) was defined by dividing the NTG values with a value derived from an exponential fit of the NTG curve of the corresponding control group. In order to compare the biological effect of the two radiation qualities, cell survival curves were established, by plotting the mean value

(from day 8 to day 23) of ACS for each tumor as a function of its corresponding absorbed dose. From exponential fits of these curves, doses required for 37% survival (D37) were derived and the RBE of At-211 was calculated by the dividing D37 for Co-60 with that of At-211.

Results: At irradiation, 10 to 14 days after inoculation, the initial tumor volume was approximately 100 mm^3. The biodistribution study showed high tumor uptake of the immunoconjugate (>10%IA/g, 3 to 21 h post injection) reaching a plateau of 14%IA/g after 7 hours. At 40 h less than 1%IA/g was found in the blood and the tumor-to-blood ratio maximized at 6.2. The administered activities of At-211 corresponded to tumor absorbed doses of 1.35, 2.65 and 3.70 Gy. The D37 value was 1.59 ($\pm$0.08) Gy. Tumor growth following Co-60 external irradiation had a D37 of 7.65 ($\pm$1.0) Gy. The corresponding RBE of At-211 irradiation was 4.8 ($\pm$0.7).

Conclusion: Using a tumor growth inhibition model in nude mice, it was possible to derive an RBE of [[211]At] alpha-radioimmunotherapy. From tumor uptake studies and MIRD dosimetry, the RBE of [211]At-RIT on tumor growth was 4.8 ($\pm$0.7).

18

INTRAPERITONEAL BETA- VERSUS ALPHA-RADIOIMMUNOTHERAPY OF DIFFUSE TYPE GASTRIC CARCINOMA: COMPARISON OF LU-177 AND BI-213 CONJUGATED TO A TUMOR SPECIFIC MAB

R Beck,[1] C Koitzsch,[1] C Seidl,[1] K Becker,[2]
C Apostolidis,[3] M Schwaiger,[1] R Senekowitsch-Schmidtke[1]
[1]Nuklearmedizinische Klinik, TU München, Munich,
Germany
[2]Institut für Pathologie, TU München, Munich, Germany
[3]Institute for Transuranium Elements, European
Commission, Karlsruhe, Germany

Objectives: Even after complete resection of solid abdominal tumors single tumor cell dissemination often causes peritoneal carcinomatosis. Currently there is no efficient treatment for this type of tumor spread. However, radioimmunotherapy of peritoneal carcinomatosis using a tumor specific MAb labeled with the short-lived (t$_{1/2}$ = 46min), high energetic (8.2 MeV; range 72 μm) alpha emitter [213]Bi displayed good therapeutic results in a nude mouse model. The purpose of this study was to evaluate the therapeutic efficiency and toxicity of the beta emitter 177Lu (t$_{1/2}$ = 6.7d, 0.13 MeV; range 670 μm) in the same model.

Methods: Nude mice were inoculated intraperitoneally (i.p.) with 10^7 human gastric cancer cells expressing mutant d9-E-Cadherin (HSC45-M2), which is specifically targeted by d9MAb but not by the unspecific control MAb (uMAb). For biodistribution studies ^{177}Lu-MAbs were injected i.p. 24 h after tumor cell inoculation. 1 h, 3 h, and 7 d after ^{177}Lu-MAb injection activity concentrations in blood and organs were quantified. For therapeutic studies mice were injected with 0.37, 1.85, 7.4 or 14.8 MBq at 24h or 8d after tumor cell inoculation. Tumor free survival was observed up to 200 days. White blood cells were counted up to 5 weeks after treatment.

Results: One hour after i.p. injection of ^{177}Lu-d9MAb the highest activity concentration was found in tumor (55%ID/g) comparable to the data obtained with [213]Bi-d9MAb. Uptake of ^{177}Lu-uMAb in the tumor was only

Large Radioimmunoliposomes for Targeted Intraperitoneal Therapy of Metastatic Cancer: Binding, Internalization and Biodistribution Studies

Stavroula Sofou, PhD[1]; Richard Enmon, PhD[1]; Stig Palm, PhD[*]; Barry Kappel, B.A.[1]; Pat Zanzonico, Ph.D.[2]; Michael R. McDevitt, PhD[1]; David A. Scheinberg, MD, PhD[1]; and George Sgouros, PhD[3].

Program in Molecular Pharmacology and Chemistry (1), Department of Radiology, Nuclear Medicine Service (2), Memorial Sloan-Kettering Cancer Center, 1275 York Ave, New York, NY 10021,
Department of Radiology (3), Division of Nuclear Medicine, Johns Hopkins Medicine, 220 Ross Research Building, 720 Rutland Ave, Baltimore, MD 21205

*Present address: Department of Radiation Physics, Göteborg University, Sweden

Key words: large immunoliposomes, trastuzumab, intraperitoneal radiotherapy, ovarian cancer

Running title: "Large immunoliposomes for radiation therapy"

ABSTRACT

Effective targeting and sterilization of intraperitoneally (IP) disseminated micrometastases remains a challenge. In this work we examine the potential of large immunoliposomes as vehicles for IP-delivery of radiation. Such radioimmunoliposomes combine the targeting efficacy of the surface-conjugated tumor-specific antibodies, with the long retention time of large liposomes in the peritoneal cavity. This could result in enhanced tumor targeting, increased tumor irradiation and minimal toxicity to normal organs.

Methods: 500 to 800 nm-diameter, zwitterionic and cationic liposomes were conjugated to trastuzumab, an anti-HER2/neu antibody. Retention of liposome content was evaluated, *in vitro*. ^{111}In-DTPA was entrapped into liposomes and the binding and internalization of radioimmunoliposomes to SKOV3, a HER2/neu-positive ovarian carcinoma cell line was examined. The biodistribution and pharmacokinetics of ^{111}In-DTPA-containing liposomes were determined by imaging and tissue counting of radioactivity in tumor-free and SKOV3-tumor-bearing mice after IP administration of the radiolabeled immunoliposomes.

Results: Large, stable, PEGylated radioimmunoliposomes of different charge were prepared. ^{111}In-DTPA was successfully and stably entrapped in liposomes. Content retention by liposomes in media and ascites fluid was high (> 53% after 20 days). *In vitro* binding of radioimmunoliposomes, after 4 hours of incubation, increased 16-fold for the zwitterionic and 53-fold for the cationic immunoliposomes compared to non-targeted liposomes. Internalized radioactivity was greater than 56% of the cell-associated radioimmunoliposomes, and depended on the type of liposomes used and the incubation

1

time. Studies, performed, *in vivo*, demonstrated the following: At four hours post-injection, tumor uptake was 17.6±3.7%ID/g and 21.3±19.5%ID/g for zwitterionic and cationic radioimmunoliposomes, respectively. Significant liver (3.9–24.9%ID/g) and spleen (130.6–296.3%ID/g) accumulation of liposomes was observed at 8 hours after administration. Fluorescent liposomes were detected in intact form in the peritoneal cavity 6 hours after administration.

Conclusions: This work demonstrates *in vitro* binding and internalization of large liposomes with prolonged intracellular retention of encapsulated radioactivity. Tumor targeting and prolonged retention following IP administration was seen, as well as significant liver and spleen accumulation. Because large radioimmunoliposomes are cleared from the peritoneal cavity relatively slowly, encapsulation of radionuclides with short half-lives would preferentially irradiate tumor cells with minimal normal organ irradiation. In addition, the high tumor targeting within the peritoneal cavity suggests that encapsulation of radionuclides with short-range emissions (e.g. alpha-particles) would spare surrounding normal tissue while delivering a sterilizing absorbed dose to disseminated peritoneal micrometastases..

INTRODUCTION

Micrometastatic dissemination in the peritoneal cavity remains a treatment challenge for patients with gastrointestinal and gynecological cancers. A promising approach for the therapy of peritoneally disseminated cancer is intraperitoneal (IP) administration of therapeutic agents. The rationale for intraperitoneal administration is twofold. First, it is a direct way to access peritoneally disseminated disease. High concentrations of the therapeutic moiety can be achieved in the peritoneal cavity, before its concentration reaches toxic levels in the dose-limiting organs [(1,2)]. Second, micrometastatic tumors in the peritoneal cavity may have not developed vasculature [(3)]. For these particular cases, intravenous administration of therapeutics will not be the optimal route to target intraperitoneal micrometastases. An effective therapy for micrometastatic tumors is of great importance because disseminated micrometastatic disease is rarely cured by current treatment options.

We studied the potential of IP administered radioimmunoliposomes for targeting and irradiation of micrometastatic cancer in the peritoneal cavity. Liposomes are closed shell structures defined by a phospholipid bilayer membrane that encloses an aqueous compartment [(4)]. We use the term 'radioimmunoliposomes' to describe those liposomes in which the internal compartment encloses radioactive elements and, the surface is conjugated with tumor-specific antibodies. Clinical trials have demonstrated that i.p.-administered radioimmunotherapy could be advantageous in cases of small volume disease [(5-7)]. Also, clinical trials on liposomally entrapped chemotherapeutic agents for i.p. therapy show encouraging results due to prolonged retention of liposomes in the peritoneal cavity [(8,9)].

3

Conjugation of multiple numbers of targeting antibodies per liposome should enhance binding of liposomes to the targeted tumor sites [(10,11)]. Because of their large size, liposomes would be expected to have extended retention in the peritoneal cavity and, consequently, to have more time to interact with tumor targets. The retention half-life in the peritoneal cavity of humans for IP administered antibodies is 30 to 67 hours (12). In contrast, the peritoneal concentration of chemotherapeutics after IP administration of their liposome based formulations, has been shown to decrease by less than 10% during the first 48 hours (9). Lastly, because the enclosed aqueous compartment of liposomes can be used to entrap up to 10^3-10^6 water soluble molecules, radiolabeling efficiency of liposomes does not present a constraint, compared to radiolabelled antibodies where high radioconjugation levels may interfere with the antibody immunoreactivity [(13)].

In this study, large radioimmunoliposomes were evaluated for targeting peritoneally disseminated tumors in an animal model of ovarian carcinoma. Ovarian cancer has the highest mortality among gynecological malignancies. Epithelial ovarian cancer, in the majority (70%) of patients, is first detected as a result of symptoms arising after the disease has spread outside of the pelvis and into the peritoneal cavity. In such cases of advanced disease (FIGO-Stage III), the 5-year survival rate employing current treatment approaches is approximately 15 to 20%. These data suggest that a new treatment modality is needed for disseminated epithelial ovarian carcinoma.

Large, PEGylated liposomes of different surface charge (zwitterionic and cationic) were engineered and indium-111, a gamma-emitting radionuclide with a 67-h half-life, was entrapped within liposomes. Liposomes were then labeled with the monoclonal antibody trastuzumab, which specifically targets the HER2/neu epidermal growth factor receptor

that is overexpressed in the SKOV3 ovarian carcinoma cell line. After characterizing the biodistribution and pharmacokinetic profile of IP administered large liposomes in tumor-free mice, the tumor uptake of radioimmunoliposomes was determined in tumor bearing mice.

Large zwitterionic and cationic anti-HER2/neu radioimmunoliposomes demonstrated rapid localization in the peritoneal tumors with higher tumor uptake than corresponding liposomes not labeled with antibodies. Also, at least 6 hours after administration, intact liposomes are still present in the peritoneal cavity. The findings of this study suggest that intraperitoneally administered large radioimmunoliposomes warrant further investigation as a potential strategy for therapy of intraperitoneal metastatic cancer.

MATERIALS AND METHODS

Reagents

The lipids L-α-phosphatidylcholine (egg) (EPC), 1,2-dipalmitoyl-sn-glycero-3-phosphoethanolamine-N-[methoxy(polyethyleneglycol)-2000] (ammonium salt) (PEG-labeled lipid), 1,2-dipalmitoyl-sn-glycero-3-ethylphosphocholine (chloride salt) (cationic lipid), L-α-phosphatidylethanolamine-N-(4-nitrobenzo-2-oxa-1,3-diazole) (egg) (NBD-PE), L-α-phosphatidylethanolamine-N-(lissamine rhodamine B sulfonyl) (egg) (rhodamine-PE), 1,2-distearoyl-sn-glycero-3-phosphoethanolamine-N-[maleimide (polyethylene glycol) 2000] (ammonium salt) (maleimide-PE) (purity >99%) were purchased from Avanti Polar Lipids (Alabaster, Al). Cholesterol, phosphate buffered saline (PBS), fluorexon (calcein), Sephadex G-50, diethylenetriaminepentaacetic acid (DTPA), 8-hydroxyquinoline (oxine), ascorbic acid, Triton X-100, and the control ascites fluid from murine myeloma were purchased from Sigma-Aldrich (St. Louis, MO). Dithionite (sodium hydrosulfite, tech. ca. 85%) was obtained from Acros Organics (NJ). Traut's reagent (2-Iminothiolane-HCl) was purchased from Pierce (Rockford, IL). Indium-111 was obtained from PerkinElmer Life Sciences Inc. (Boston, MA).

Liposome preparation

Mixtures of phosphatidyl choline (EPC), cholesterol (1:1 molar ratio), and PEG-labeled lipids (5.3 mole % of total lipid) in $CHCl_3$ were dried in a rotary evaporator (for cationic liposomes, cationic lipid was included in 10 mole % of total lipid). For stability measurements, the lipids were resuspended in calcein solution (55 mM calcein in phosphate buffer, isosmolar to PBS, pH=7.4). For ^{111}In passive entrapment, the lipids

6

were resuspended in PBS containing chelated indium complexes (^{111}In-DTPA, 3.7-37 MBq per ml). The lipid suspension was then annealed to 55°C for 2 hours [(14)]. To make liposomes, the lipid suspension was then taken through twenty-one cycles of extrusion (LiposoFast, Avestin, Ontario, Canada) through two stacked polycarbonate filters (800 nm filter pore diameter), and unentrapped contents were removed by size exclusion chromatography (SEC) in a Sephadex G-50 (Aldrich, St. Louis, MO) packed 1x10 cm column, eluted with a PBS isotonic buffer. For ^{111}In encapsulating liposomes, 1mM DTPA was added to the liposome suspension 30 minutes prior to SEC. Also, a chemical method was followed to load ^{111}In into preformed liposomes. The loading protocol for indium is published elsewhere [(15)]. Briefly, to 1 ml of preformed liposomes, with entrapped 2mM DTPA, we added drop-wise 100 µl of InCl$_3$ in 3 mM HCl and 100 µl of oxine in 1.8 wt % NaCl / 20mM sodium acetate (3 µl of 11 mM oxine in EtOH added to the acetate buffer, pH=5.5). After loading, unentrapped ^{111}In was complexed with externally added 2mM EDTA and was separated from the liposomal suspension by SEC in a Sephadex G-50 packed 1x10 cm column, eluted with phosphate buffer (PBS, pH=7.4). Ascorbic acid (8 mmol/l) was coentrapped to minimize lipid oxidation due to radiation.

Retention of entrapped contents by liposomes

To study the retention of entrapped contents by liposomes, a fluorescent dye (calcein) was encapsulated at self-quenching concentrations. Liposome stability was determined in PBS, in RPMI 1640 medium supplemented with 1-10% fetal calf serum (Sigma-Aldrich), and in murine ascites fluid (Sigma-Aldrich) at 37°C over time. The

fluorescence intensity of liposome suspensions was measured by a fluorescence microplate reader (ex: 485 nm; em: 538 nm). Destabilization of the liposomal membrane causes calcein leakage from the liposomes. Calcein leakage is followed by dilution of calcein into the surrounding solution and relief of the fluorescence self-quenching effect, which results in increase of fluorescence intensity. To normalize and properly compare different samples, Triton X-100 (4.5% wt /wt) was added into the suspension to achieve complete calcein release. To quantitate liposome stability, the fluorescence self-quenching efficiency q of liposome suspensions was compared over the period of 30 days ($q=I_{max}/I$, where I is the measured fluorescence intensity before Triton X-100 addition, and I_{max} the maximum fluorescence intensity after Triton X-100 addition).

To determine the retention of ^{111}In by liposomes, DTPA was added for 30 minutes into a fraction of the liposome suspension, and after SEC, the γ-emissions of ^{111}In retained by liposomes were measured using a Cobra γ-counter (Packard Cobra Gamma Counter, Packard Instrument Co., Inc., Meriden, CT). The energy window used for ^{111}In was 15-550 keV.

Liposome lamellarity

A dithionite assay was used to determine the lamellarity of the zwitterionic and cationic liposomes. Dithionite ion $S_2O_4^-$ and the spontaneously produced $\cdot SO_2^-$ radical react with the NBD-PE labeled lipids of the outer membrane layer and produce non-fluorescent derivatives (McIntyre and Sleight, 1991). They diffuse very slowly through the bilayer and thus allow the quantitative distinction of the inner and outer layer lipids. In our NBD-

PE labeled vesicle preparations unilamellarity was verified by a 53 ± 0.1 % (zwitterionic liposomes) and 52 ± 0.2 % (cationic liposomes) decrease of the initial fluorescence upon dithionite addition.

Liposome size distribution determination

Dynamic light scattering (DLS) of liposome suspensions was studied with an N4 Plus autocorrelator (Beckman-Coulter), equipped with a 632.8 nm He-Ne laser light source. Scattering was detected at 15.7°, 23.0°, 30.2°, and 62.6°. Particle size distributions at each angle were calculated from autocorrelation data analysis by CONTIN [(16)]. The average liposome size was calculated to be the y-intercept at zero angle of the measured average particle size values vs $\sin^2(\theta)$ [(17)]. All buffer solutions used were filtered with 0.22 μm filters just prior to liposome preparation. The collection times for the autocorrelation data were 1-4 minutes.

Liposome immunolabeling

Trastuzumab (5-10 mg/ml, in PBS, pH=8) was purified from Herceptin® (Genentech, South San Francisco, CA) and was reacted with Traut's reagent for 1 hr at room temperature under a nitrogen atmosphere. Then the antibody was purified by size exclusion chromatography in a 10DG column (Biorad, Hercules, CA) eluted with PBS (with 1mM EDTA, pH=7.4). An average of 5-7 sulfhydryl groups per antibody were determined using the Ellman's assay and a protein assay (DC protein assay, Biorad). Liposomes (7-15 mM lipid) containing maleimide-PE (1 mole% of total lipid) were then incubated with antibody solution (0.5-5 mg/ml) overnight at room temperature under N_2.

After completion of conjugation, excess maleimide groups were quenched with β-mercaptoethanol (3:1 molar ratio) for 30 minutes. Immunoliposomes were purified from unreacted antibody and β-mercaptoethanol by size exclusion chromatography in a 4B stationary phase (Sigma-Aldrich) packed 1x10 cm column, eluted with PBS. A protein assay was used to quantify the concentration of antibodies in the liposome suspension. Lipid concentration was determined by the fluorescence intensity of rhodamine-PE containing liposomes (0.5-1 mole% of total lipid). The average number of antibodies per liposome was estimated using the assumption that for 650 nm diameter liposomes, and 70Å^2 head group surface area per lipid [(18)], a liposome would consist of an average of 3.7 million lipid molecules.

Cell culture and Tumor inoculation

Stock T-flask cultures of the human ovarian carcinoma cell line SKOV3-NMP2 [(2)] were propagated at 37°C, in 5% CO2 in RPMI 1640 media supplemented with 10% fetal calf serum (Sigma-Aldrich), 100 units/ml penicillin, and 100mg/ml streptomycin. Cell concentration was determined by counting trypsinized cells with a hemocytometer. Tumor inoculation was prepared from a single cell suspension in DME medium (Dulbecco's Modified Eagle's Medium). Each 4-6 week old female Balb/c nude mouse (Taconic, Germantown, NY) received 0.15-0.20 ml inoculum of 5x10^6 cells administered by intraperitoneal injection.

Mice were housed in filter top cages and provided with sterile food and water. Animals were maintained according to the regulations of the Research Animal Resource Center

(RARC) at Memorial Sloan-Kettering Cancer Center (MSKCC), and animal protocols were approved by the Institutional Animal Care and Use Committee (IACUC).

Cell Binding and internalization of liposomes

Flow cytometry was used to determine the specific binding of liposomes to SKOV3 cells. The liposomal membrane was labeled with the fluorescent lipid rhodamine-PE (excitation: 550 nm; emission: 590 nm). Harvested SKOV3 cells were washed three times with ice-cold buffer (PBS/ 0.5% BSA/ 0.02% NaN$_3$) and then resuspended at a density of 5.6×10^6 cells/ml. 10^6 cells were incubated on ice with liposomes for 25 minutes (3.3 mM final lipid concentration), then washed three times and finally resuspended at a density of 2.5×10^6 cells/ml. To determine the extend of specific binding of immunoliposomes to the HER2/neu antigen receptor, cells were also preincubated with trastuzumab at 5μg of antibody per one million cells for 25 minutes on ice. Cells were then washed twice with ice-cold buffer and incubated with liposomes as above. Fluorescence counting of cell suspensions was measured using a Beckman-Coulter Cytonics FC500 flow cytometer (Fullerton, CA), and analyzed with the software FlowJo (Tree Star, Inc., Ashland, OR).

To quantitate cell binding and internalization of liposomes, harvested SKOV3 cells were washed twice with ice-cold media (RPMI 1640/ 10% FBS/ 2% BSA) and then resuspended in cold media (as above) at a density of 10^6 cells/ml. Radiolabeled liposomes (250 μl of 1.8mM lipid) were added to 3.5 ml of cell suspension and two 200μl samples were immediately taken and processed as described below. The cells were then placed in a humidified, 37°C incubator with 5% CO$_2$, where they were periodically

swirled and sampled at 0.5, 1, 2, 4, and 24 hrs. The cells were washed three times with 2ml of ice-cold PBS, and then 1ml of an acidic striping buffer (50 mM glycine, 150 mM NaCl, pH=2.8) was added for 10 minutes at room temperature to eliminate the charge-specific binding of membrane bound conjugates and to remove the surface bound immunoliposomes. After centrifugation, the supernatant and pellet were counted, and the percentages of membrane-bound and internalized counts were determined.

Excised organ quantitation

Mice were injected IP with liposomes (0.1-0.2 ml suspension, 1.4 μmole total lipid) with entrapped ^{111}In, and were sacrificed at different time points post-injection by CO_2 intoxication for dissection. The average activity per inoculum was 37 kBq. The whole body clearance was measured with a dose calibrator (Model CRC-15R, Capintec, NJ). Blood was collected via cardiac puncture. Organ and muscle tissues were washed in PBS and weighed. The samples were then counted for photons in a gamma-counter. Results were expressed for each organ as percentage of total radioactivity injected, divided by the organ mass (%ID/g). A bi-exponential curve of the form $A_1*exp(-t*ln(2)/T_1))-A_2*exp(-t*ln(2)/T_2))$ was applied to fit the uptake and clearance phase of the blood kinetics, using a commercial software program (SigmaPlot,, SPSS Inc.).

Gamma camera imaging

Mice were injected intraperitoneally with 0.1-0.4 ml liposome suspensions with encapsulated ^{111}In and average activity per inoculum 0.74-1.48 MBq. Each mouse was imaged with a planar gamma camera using the small-animal X-SPECT Imaging system

(Gamma Medica Inc., Northridge, CA). Time dependent distribution and localization of liposomes were determined by four imaging sessions over the course of 24 hours. During imaging, the mice were kept anesthetized using an isoflurane (Forane) (Baxter, Deerfield, IL) loaded vaporizer.

Mice fluorescent imaging

To image intact liposomes in the peritoneal cavity, mice were injected with liposomes containing an encapsulated fluorophore (calcein) at self-quenching concentrations. Mice were anesthetized at 6 or 48 hours post-injection using 100 mg/kg ketamine, 10 mg/kg xylazine, and were then sacrificed by cervical dislocation. The peritoneal cavity was exposed after removal of the abdominal skin and the peritoneal membrane, and fluorescent images of the peritoneal cavity were acquired before and after addition of Triton X-100, which disrupts the liposomal membranes and causes relief of calcein self-quenching. Mice were digitally imaged using an ORCA CCD camera fitted with a macro-lens (Hamamatsu, Hamamatsu City, Japan) and MCID 5+ imaging software (Imaging Research, Ontario, Canada). Two mice were imaged per time point for each of the two liposome suspensions injected (zwitterionic, cationic). Fluorescent images were acquired using an Illunatool Tunable Lighting System, 470nm +/- 20nm exciter filter and 525nm +/- 20nm barrier filter (Lightools, Encinitas, CA).

RESULTS

Liposome characterization

The measured average liposome sizes for the zwitterionic composition was 646 ± 288 nm (diameter) on the day of preparation and 657 ± 365 nm after 30 days. For the cationic composition the corresponding values were 602 ± 385 nm and 678 ± 357 nm, respectively. DISCUSS REASON FOR CHANGE AT SOME POINT – IS IT FUSION OVER TIME?

To evaluate the stability of liposomes over time, in terms of content retention, calcein (a self-quenching fluorophore) was entrapped into liposomes at high concentrations. Release of calcein, due to membrane instability, results in dilution of the fluorophore by the surrounding solvent, relief of self-quenching, and increase of the fluorescence intensity. The fractional fluorescence self-quenching decrease, $\Delta q \times 100$, is shown on tables 1 and 2 for zwitterionic and cationic liposomes over the period of 30 days at $37^{\circ}C$ in media (with 1-10% serum) and in ascites fluid, respectively. Incubation of liposomes in media resulted, after the first 24 hours, in a maximum of 17% decrease in self-quenching, which possibly could be attributed to differences in osmolarity between the encapsulated calcein solution and the liposome surrounding solvent. Beyond this point liposomes were generally stable for over 30 days (Table 1). In ascites fluid, after 15 days of incubation, a 21% decrease in self-quenching was measured for zwitterionic liposomes, and no decrease was observed for cationic liposomes. After incubation for 30 days in ascites fluid, more than 50% decrease in self-quenching was observed for both zwitterionic and cationic liposomes.

Retention of ^{111}In by liposomes

The efficiency of ^{111}In entrapment in liposomes was 5-10% and 73-81% with the passive
and chemical loading method, respectively.

The decay-corrected ^{111}In activity that was retained in the zwitterionic and cationic
liposomes three days after preparation was >88% and > 87% of the liposome initial
activity (on the day of preparation) for the liposomes that were loaded with the passive
and chemical method, respectively.

Liposome immunolabelling

The conjugation reaction resulted in 65-90 antibodies per zwitterionic liposome and 90-
145 antibodies per cationic liposome. To determine the possible leakage of entrapped
contents during conjugation, calcein was encapsulated into liposomes at self-quenching
concentrations. No significant change in self-quenching efficiency was detected (data not
shown).

Cell binding and internalization of liposomes

To determine binding of liposomes to SKOV3 cells, the liposomal membrane was labeled
with a fluorescent phospholipid (rhodamine-PE, 1 mole % of total lipid), and cell
suspensions were incubated with immunolabeled and plain liposomes. Also, in parallel
measurements for the determination of the specific binding of immunoliposomes to the
HER2/neu antigen receptor, SKOV3 cells were previously blocked with excess
trastuzumab, the antibody that was also conjugated to immunoliposomes. Figures 1A and
1B show the flow cytometry histograms for binding of zwitterionic immunoliposomes

and plain liposomes to SKOV3 cells, respectively, with (shaded gray) and without

blocking (thick solid line) of the HER2/neu antigen receptor on the cell surface. A

significant shift in fluorescence counts of SKOV3 cells was detected only in the case of

immunoliposomes, and only when the HER2/neu receptors on the cell surface were not

blocked (Figure 1A, thick solid line). Non-specific binding of plain zwitterionic

liposomes to SKOV3 cells was not detected as is depicted by the unchanged fluorescence

of cells in Figure 1B. Contrary to zwitterionic liposomes, cationic liposomes exhibit non-

specific binding (Figure 1C: shaded gray, and Figure 1D: shaded gray and thick solid

line). Binding of cationic immunoliposomes to unblocked SKOV3 cells showed the

largest shift in cell fluorescence counts (Figure 1C: thick solid line).

SKOV3 cells were also incubated with TRIC-labeled antibodies. Trastuzumab® (shaded

black) but not Rituximab® (an irrelevant antiCD20 antibody, shaded gray) binds

specifically to SKOV3 cells, as is shown in Figure 1E.

To quantitatively determine liposomal binding and internalization, liposomes with

entrapped ^{111}In were incubated at 37°C with SKOV3 cell suspensions for 0, 0.5, 1, 2, 4

and 24 hours. The total cell-associated radioactivity increased over time of incubation

reaching at 4 hours a 4-fold increase for zwitterionic immunoliposomes (Figure 2A) and

a 29-fold increase for cationic immunoliposomes (Figure 2B) compared to the values for

total cell-associated radioactivity of immunoliposomes at t=0. For zwitterionic

immunoliposomes, internalized radioactivity increased 13-fold within the first 4 hours

and then remained constant for up to 24 hours (24 hr. time-point not shown on plot).

However, the total cell associated intensity continued to rise reaching a 6-fold increase

after 24 hours. In other words, internalization and replacement on the cell membrane of

the HER2/neu target receptor occurred only the first few hours of incubation. At later times, internalization of the receptor was diminished.

For cationic immunoliposomes, both the total cell-associated radioactivity and the internalized radioactivity increased over 24 hours of incubation (24 hour time point not shown on the plot). No saturation of receptor internalization was observed. At 24 hours, a 189-fold increase in cell-associated radioactivity was observed with a 111-fold increase in internalized counts. The increase in membrane bound activity implies that the HER2/neu target receptor was being replaced on the cell membrane after receptor internalization.

At 24 hours, 1.2% of the total zwitterionic and 13.3% of the total cationic immunoliposome activity was cell-associated. Non-targeted plain liposomes showed low, non-specific, cell-binding (Figures 2A and 2B). Only 0.3% of total zwitterionic and 0.9% of total cationic non-targeted liposome activity was cell-associated.

Biodistributions of large liposomes in tumor free mice

The biodistributions and pharmacokinetics of large zwitterionic and cationic plain liposomes, with entrapped ^{111}In-DTPA, were determined, initially, in Balb/c mice without tumor. At 1, 4, 8, and 24 hours post IP administration of liposomal suspensions, animals were killed and the radioactivity distribution of excised tissues was obtained by γ counting. The biodistributions of large zwitterionic and cationic plain liposomes in mice without tumor are shown in Figures 3A and 3B respectively. The most significant normal organ accumulation was in the liver and spleen. 4 hours post-injection of zwitterionic liposomes (Figure 3A), $3.2 \pm 1.3\%$ ID/g and $68.8 \pm 40.1\%$ ID/g was accumulated in the

liver and spleen, respectively, and at 8 hours the corresponding values were $3.9 \pm 3.5\%$ ID/g and $130.6 \pm 197.9\%$ ID/g. Cationic liposomes had higher uptake by the liver (Figure 3B). At 4 and 8 hours post-injection $11.2 \pm 7.7\%$ ID/g and $24.9 \pm 4.5\%$ ID/g of cationic liposomes was accumulated in the liver. The maximum uptake in the liver and spleen was observed 8 hours post-injection for both liposomal compositions.

The whole body clearance was low when liposomes were administered GIVE NUMBER(S). On the contrary, rapid whole body clearance was observed after administration of ^{111}In-DTPA (Figure 3C). Blood uptake and elimination kinetics of zwitterionic liposomes was described by a bi-exponential curve with mean half-lives of 0.51 ± 0.29 hours and 5.79 ± 0.24 hours, respectively. The corresponding values for cationic liposomes were 0.68 ± 0.84 hours and 2.74 ± 0.71 hours. At early time (1-4 hours), blood showed a significant uptake of 6-8% ID/g that may reflect a fraction of rapidly disrupted liposomes after intraperitoneal injection, or smaller size liposomes that escape the peritoneal cavity through lymphatic drainage.

Biodistributions of large zwitterionic liposomes in tumor bearing mice

Biodistributions of plain- and immuno- liposomes were determined in tumor bearing mice. Fourteen days after inoculation, a tumor pattern was formed, that consisted of nodules on the ventral side of the spleen. Smaller nodules ($\sim$ 1mm in diameter) were frequently observed within the mesentery. At 14 days post-innoculation, the mean weight of observed tumor nodules was 0.269 ± 0.242 g (n=30, total number of animals).

4 hours after IP administration of large zwitterionic liposomes the tumor uptake of immunoliposomes was $17.6 \pm 3.7\%$ ID/g, and $2.7 \pm 0.7\%$ ID/g for plain non-targeted

liposomes (Figures 4A and 4B). Twenty-four (SPELL OUT No.s AT START OF SENTENCE) hours after administration, the difference in tumor uptake between the two liposomal groups was smaller: $12.0 \pm 4.0\%$ ID/g for immunoliposomes and $8.7 \pm 6.1\%$ ID/g for plain zwitterionic liposomes. The normal organ with the highest uptake was the spleen with $83.3 \pm 19.7\%$ ID/g for zwitterionic immunoliposomes. For non-targeted liposomes the spleen uptake at 4 hours was $33.9 \pm 29.4\%$ ID/g, and at 24 hours it reached the value of $82.5 \pm 49.1\%$ ID/g. Liver had the second highest normal organ uptake. 4 hours after administration, $9.1 \pm 0.4\%$ ID/g of immunoliposomes and $5.0 \pm 1.7\%$ ID/g of plain zwitterionic liposomes were observed in the liver. After 24 hours, the liver uptake increased to $14.1 \pm 2.2\%$ ID/g and $11.1 \pm 2.3\%$ ID/g for immunoliposomes and plain non-targeted liposomes, respectively. Kidney uptake was insignificant.

Biodistributions of plain zwitterionic liposomes in mice with and without tumor had no significantly different uptake by the spleen and liver.

Biodistributions of large cationic liposomes in tumor bearing mice

Large cationic liposomes demonstrated a tumor uptake pattern similar to zwitterionic liposomes (Figures 5A and 5B). Four hours after IP administration, tumor uptake was $21.3 \pm 19.5\%$ID/g for cationic immunoliposomes, and $7.1 \pm 2.5\%$ ID/g for plain cationic liposomes; 24 hours after administration, the difference in tumor localization between immunoliposomes ($21.7 \pm 14.3\%$ ID/g) and plain liposomes ($18.6 \pm 12.9\%$ ID/g) was not significantly smaller as observed for zwitterionic liposomes. Spleen uptake increased with time and 24 hours post-injection it reached the value of $148.7 \pm 67.2\%$ ID/g and $161.5 \pm 104.0\%$ ID/g for cationic immunoliposomes and non-targeted liposomes,

20

respectively. Liver uptake, 4 hours post-injection, was $12.9 \pm 11.3\%$ ID/g for

immunoliposomes and $10.0 \pm 6.5\%$ ID/g for plain non-targeted liposomes. 24 hours later,

it further increased to $21.4 \pm 7.8\%$ ID/g and $16.9 \pm 7.2\%$ ID/g for cationic

imunoliposomes and plain liposomes, respectively. Kidney uptake was not significant.

Blood uptake was low.

The biodistributions of plain cationic liposomes were similar in tumor bearing and tumor

free mice, except for the spleen uptake that was significantly higher in the latter.

Blood uptake for all types of liposomes was between 2.7-8.0% ID/g at 4 hours and

dropped to below 0.8% ID/g at 24 hours. Liver and spleen uptake of the cationic

radioimmunoliposomes was greater than the corresponding values for zwitterionic

immunoliposomes. Both immuno-liposomal compositions showed similar tumor uptake 4

hours after administration.

Imaging of liposomes in vivo

The distribution of ^{111}In-DTPA entrapping liposomes in mice after IP administration was

imaged using a planar gamma-camera (Figure 6). No radioactivity into the circulation

was observed, as is shown by the absence of radiation intensity in the cardiac region. The

images suggest that liposomes are retained intact in the peritoneal region, since the native

distribution of free ^{111}In-DTPA was not observed.

Fluorescence imaging of liposomes in the peritoneal cavity

To verify the presence of intact liposomes in the peritoneal cavity at later times after

administration, large PEGylated liposomes with an encapsulated fluorophore (calcein), at

self-quenching concentrations, were injected intraperitoneally in mice. Six hours later,

the animals were sacrificed, the abdominal cavity was exposed and the peritoneal

membrane was removed. To detect any intact liposomes in the peritoneal cavity, Triton-X

100 was added to disrupt the intact structures, release calcein from the liposomes, relax

self-quenching, and thereby increase the fluorescence intensity. The fluorescence images

of the peritoneal cavities of mice are shown in Figures 7A and 7B for animals that were

injected with zwitterionic and cationic liposomes, respectively, before the addition of

Triton-X 100 (Figures 7A(i) and 7B(i)). After addition of the lipid solubilizer, dramatic

increase of fluorescence in the peritoneal fluid was observed for both animals, indicating

that 6 hours after IP administration of liposomes, there are still intact liposomes in the

peritoneal fluid (Figures 7A(ii) and 7B(ii)).

Mice that were administered fluorescent liposomes were also imaged 48 hours post-

injection (data not shown). Intact zwitterionic and cationic liposomes were observed only

in the mesentery, as verified by enhancement of the fluorescence intensity after Triton-X

100 addition.

DISCUSSION

Disseminated micrometastatic disease is usually incurable. Peritoneal dissemination is frequent in advanced colorectal and gynecologic cancers. Intraperitoneal administration of therapeutics for targeting peritoneal micrometastatic disease has the advantage of direct tumor access and may allow high tumor accumulation of therapeutics to be achieved before uptake levels in normal organs becomes a limiting factor. Also, because the onset of tumor vasculature development usually starts after a certain tumor size is reached, this route of administration is optimal for therapy of intraperitoneal micrometastases, which will not have developed vasculature.

Towards this goal, we developed large radioimmunoliposomes and studied their potential to target tumors in the peritoneal cavity. We use the term radioimmunoliposomes to define the liposomal structures that contain encapsulated radionuclides and, are conjugated, on their membrane, with tumor-targeting antibodies. In principle, radioimmunoliposomes have the potential to combine the targeting advantages of radioimmunotherapy, namely (a) specific tumor targeting, (b) enhanced tumor irradiation, and (c) minimal normal organ toxicity, with the delivery characteristics of liposomes, which include (a) vast internal volume for encapsulation of radioisotopes, and (b) considerable surface area for multivalent targeting-ligand conjugation. Over the last years, steric stabilization of liposomes [(11)] has resulted in reduction of their uptake and catabolism by the reticuloendothelial system, and, thus, has enabled their application in drug delivery. Liposomal encapsulation alters the pharmacokinetics of IP administered agents which are cleared rapidly from the peritoneum through peritoneal membrane

absorption, but, instead, follow the slower clearance of liposomes through lymphatic drainage.

Large zwitterionic and cationic PEGylated liposomes (650 nm in diameter) were prepared and characterized for content leakage (calcein release) and size (DLS) over time. Liposomes were stable during a period of 20 days in ascites fluid and in media (1-10% serum) at $37^{o}C$.

Liposomes were immunolabeled with the antiHER2/neu monoclonal antibody trastuzumab with an efficiency of 65-95 antibodies per zwitterionic liposome and 95-130 antibodies per cationic liposome. Enhanced specific binding of immunoliposomes to the HER2/neu antigen receptor of the human ovarian carcinoma cell line SKOV3 was demonstrated by flow cytometry. Non specific binding was not detected for the zwitterionic liposomes. Cationic immunoliposomes associated with cells to some extent even after blocking of the antigen receptor, probably due to electrostatic interactions between the positively charged liposomal membrane and the locally negatively charged cell membrane [(20)]. Similarly, non-specific binding was also observed for the plain non-targeted cationic liposomes. The increased binding of cationic immunoliposomes (mean shift = 74) compared to zwitterionic immunoliposomes (mean shift = 59) could be explained not only by the non-specific electrostatic interactions of the first, but also by the higher surface-density of antibodies on cationic liposomes.

Quantification of binding and internalization of liposomes to SKOV3 cells was determined using liposomes with encapsulated ^{111}In-DTPA. Both zwitterionic and cationic immunoliposomes rapidly bound and internalized into SKOV3 ovarian carcinoma tumor cells. After 4 hours of incubation, the fraction of internalized activity

was >55% and >66% of the total cell-associated activity for zwitterionic and cationic immunoliposomes, respectively. Saturation of the internalization mechanism, after 4 hours of incubation, was observed only for zwitterionic immunoliposomes and not for cationic immunoliposomes. Since the cationic immunoliposome-cell interaction includes a substantial non-specific component, we speculate that this non-specific and possibly non-saturable component is also operative for internalization. Total cell-associated activity of cationic immunoliposomes was more extensive 10-fold more than zwitterionic immunoliposomes, and it increased throughout the period of 24 hours.

Similar binding and internalization curves for both types of immunoliposomes were obtained when liposomes with higher surface-density of conjugated antibodies were used (data not shown). Minimal cell association *in vitro* was observed with plain non-targeted zwitterionic and cationic liposomes.

Spleen and liver uptake are considered significant features of liposomal biodistribution, *in vivo*. To effectively target and irradiate peritoneally disseminated micrometastases, we developed large radioimmunoliposomes that can rapidly target tumors after IP administration, and studied the kinetics of their accumulation to the spleen and liver. Because the maximum uptake by those organs is reached a few hours after administration, to minimize the toxicity effects to the spleen and liver, we propose liposomal entrapment of radionuclides with half-lives shorter than this time frame. Also, intravenous pre-injection of unlabeled plain liposomes could be used to saturate these sites *(19)*. It is of major importance, however, that the large liposomes we studied showed no significant blood and kidney uptake. In addition, due to the high number of

25

radionuclei encapsulated per liposome, high radiation dose per liposome can be delivered at the tumor site.

Encapsulated ^{111}In-DTPA was used that allows for animal imaging and quantitation of the radioactivity of the excised organs. The highest normal organ accumulation was observed in the liver and spleen. The maximum uptake was observed 8 hours post-injection for both liposomal compositions. The gamma camera images of the animals suggested peritoneal retention of liposomes and did not show detectable increase in the blood pool concentration or in the kidney uptake. Peritoneal retention of intact liposomes was directly confirmed, 6 hours after IP administration, by fluorescence imaging and relief of self-quenching of calcein encapsulating liposomes. 48 hours later, only a few intact liposomes were detected in the mesenteric region by the same method.

The tumor targeting efficiency of immunoliposomes *in vivo* showed that immunolabeling of liposomes results in enhancement of tumor targeting at short times (4 hours post-injection), demonstrated by a 6.5-fold increase in tumor uptake between zwitterionic immunoliposomes and zwitterionic plain liposomes, and a 3-fold increase for the cationic composition. At later times (24 hours post injection), the difference in tumor uptake between immunoliposomes and plain liposomes was less significant. Cationic immunoliposomes showed higher mean tumor uptake than zwitterionic immunoliposomes, but this result may be due to the moderately different numbers of conjugated antibodies per liposome between the two types of immunoliposomes. The tumor uptake values for plain liposomes were significant, and were in contrast to their minimal cell binding that was observed *in vitro*. Tumor uptake of plain cationic

liposomes was higher compared to plain zwitterionic liposomes, which was in accordance with the flow cytometry observations.

The SKOV3 ovarian carcinoma animal model and the IP administered antiHER2/neu large radioimmunoliposomes were selected as a proof of principle for effective targeting of tumors in the peritoneal cavity for potential radionuclide therapy of micrometastatic dissemination. *In vitro* studies showed that after cell binding large radioimmunoliposomes were internalized to a significant extent. Immunolabeled liposomes showed rapid and increased tumor uptake before the maximum liver concentrations were reached. Because of those two characteristics of the radioimmunoliposomes studied, we propose their potential application in IP radiotherapy of micrometastases with entrapped emitters of short-range and short half-life. Alpha-particle emitters might be the most appropriate, since the range of alpha-particles (50-80 μm) is relatively short and should not cause significant abdominal radiotoxicity due to the prolonged retention of liposomes in the peritoneal cavity. The alpha-emitters such as ^{211}At ($t_{1/2}$=7.21 hours) or ^{213}Bi ($t_{1/2}$=45 min) are promising candidates, because they will have significantly decayed by the time the maximum normal organ uptake will be achieved.

Conclusion

We have engineered large antiHER2/neu radioimmunoliposomes that can rapidly and effectively target intraperitoneal tumors in an ovarian carcinoma animal model. Large liposomes are intact in the peritoneal cavity for hours after IP administration, and accumulate to normal organs (liver and spleen) with relatively low rates. *In vitro*, large radioimmunoliposomes bind and internalize into SKOV3 cells to a significant extent. Large radioimmunoliposomes, with encapsulated short-half life, short-range emitters, are potential agents for the therapy of (or prophylaxis against) peritoneal micrometastatic disease.

Acknowledgements

References

1. Buijs WCAM, Tibben JG, Boerman OC, Molthoff CFM, Massuger LFAG, Koenders EB, Schijf CPT, Siegel JA, Corstens FHM. Dosimetric analysis of chimeric monoclonal antibody cMOv18 IgG in ovarian carcinoma patients after intraperitoneal and intravenous administration. *Eur. J. Nucl. Med.* 1998; 25: 1552-1561.

2. Borchardt P, Yuan R, Miederer M, McDevitt M, Scheinberg D. Targeted actinium-225 in vivo generators for therapy of ovarian cancer. Cancer research. Volume 63; 2003. p 5084-5090.

3. Li C-Y, Shan S, Huang Q, Braun RD, Lanzen J, Hu K, Lin P, Dewhirst MW. Initial Stages of Tumor Cell-Induced Angiogenesis: Evaluation Via Skin Window Chambers in Rodent Models. *J Natl Cancer Inst.* 2000; 92: 143-147.

4. Cullis PR, DeKruijff B. Lipid polymorphism and the functional role of lipids in biological membranes. *Biochim. Biophys. Acta.* 1979; 559: 399-420.

5. Epenetos A, Munro A, Stewart S, Rampling R, Lambert H, McKenzie C, Soutter P, Rahemtulla A, Hooker G, Sivolapenko G. Antibody-guided irradiation of advanced ovarian cancer with intraperitoneally administered radiolabeled monoclonal antibodies. *J Clin Oncol.* 1987; 5: 1890-1899.

6. Crippa F, Bolis G, Seregni E, Gavoni N, Scarfone G, Ferraris C, Buraggi GL, Bombardieri E. Single-dose intraperitoneal radioimmunotherapy with the murine monoclonal antibody I-131 MOv18: Clinical results in patients with minimal residual disease of ovarian cancer. *European Journal of Cancer.* 1995; 31: 686-690.

7. Meredith R, Partridge E, Alvarez R, Khazaeli M, Plott G, Russell C, Wheeler R, Liu T, Grizzle W, Schlom J and others. Intraperitoneal radioimmunotherapy of ovarian cancer with Lutetium-177-CC49. J Nucl Med. Volume 37; 1996. p 1491-1496.

8. Delgado G, Potkul R, Treat J, Lewandowski G, Barter J, Forst D, Rahman A. A phase I/II study of intraperitoneally administered doxorubicin entrapped in cardiolipin liposomes in patients with ovarian cancer. Am J Obstet Gynecol. Volume 160; 1989. p 812-817.

9. Verschraegen C, Kumagai S, Davidson R, Feig B, Mansfield P, Lee S, Maclean D, Hu W, Khokhar A, Siddik Z. Phase I clinical and pharmacological study of intraperitoneal cis-bis-neodecanoato(trans- R, R-1, 2-diaminocyclohexane)-platinum II entrapped in multilamellar liposome vesicles. J Cancer Res Clin Oncol. Volume 129; 2003. p 549-555.

10. Kirpotin DB, Park JW, Hong SK, Zalipsky S, Li W-L, Carter P, Benz CC, Papahadjopoulos D. Sterically stabilized anti-HER2 immunoliposomes: design and targeting to human breast cancer cells *in vitro*. *Biochemistry*.1997; 36: 66-75.

11. Sapra P, Allen TM. Ligand-targeted liposomal anticancer drugs. *Progress in Lipid Research*.2003; 42: 439-462.

12. Junghans RP, Sgouros G, Scheinberg DA. Andibody-based immunotherapies for cancer. In: Chabner BA, Longo DL, editors. Cancer Chemotherapy and Biotherapy. Philadelphia: Lippincott-Raven Publishers; 1996. p 678.

13. Nikula TK, Bocchia M, Curcio MJ, Sgouros G, Ma Y, Finn RD, Scheinberg DA. Impact of the high tyrosine fraction in complementarity determining regions: measured

and predicted effects of radioiodination on IgG immunoreactivity. *Molecular Immunology*.1995; 32: 865-872.

14. Castile JD, Taylor KMG. Factors affecting the size distribution of liposomes produced by freeze-thaw extrusion. *Int. J. Pharm.*1999; 188: 87-95.

15. Hwang KJ, Merriam JE, Beaumier PL, Luk K-FS. Encapsulation, with high efficiency, of radioactive metal ions in liposomes. *Biochim Biophys Acta*.1982; 716: 101-109.

16. Provencher SW. A constrained regularization method for inverting data represented by linear algebraic or integral equations. *Comput. Phys. Commun.*1982; 27: 213-227.

17. Teraoka I. Polymer Solutions: An Introduction to Physical Properties: John Wiley & Sons; 2002.

18. Lasic DD. Liposomes from Physics to Applications. Amsterdam: Elsevier; 1993. pp.: 555 p.

19. Drummond DD, Meyer O, Hong K, Kirpotin DB, Papahadjopoulos D. Optimizing liposomes for delivery of chemotherapeutic agents to solid tumors. *Pharmacol Rev*.1999; 51: 691-743.

20. Devaux PF. Protein Involvement in Transmembrane Lipid Asymmetry. *Annual Review of Biophysics and Biomolecular Structure*.1992; 21: 417-439.

Table 1

Retention of entrapped contents by zwitterionic and cationic liposomes in media (1-10% serum) at 37°C for 30 days.

Time [days]	Large Zwitterionic Liposomes $\Delta q \times 100*$			Large Cationic Liposomes $\Delta q \times 100*$		
	1% serum	5% serum	10% serum	1% serum	5% serum	10% serum
1	0± 9	0± 7	0± 6	0± 7	0± 7	0± 6
2	17± 9	14± 6	6± 6	2± 6	-2± 6	2± 5
3	21± 8	14± 6	8± 7	15± 7	10± 7	15± 7
14	22±10	6± 6	0± 6	32± 6	6± 6	5± 6
30	21± 9	-1± 6	-9±6	39± 6	0± 7	-5± 6

* Fractional fluorescence self-quenching decrease due to calcein leakage from PEGylated liposomes over time ($\Delta q_{day\_x}=(q_{day\_1}-q_{day\_x})/ q_{day\_1}$). After the first 24 hours a maximum of 17% in self-quenching decrease was measured for all liposomes (possibly due to differences in osmotic pressure across the liposomal membrane). Beyond this point all liposomes were generally stable for over 30 days. The uncertainties correspond to standard errors of repeated measurements.

Table 2

Retention of entrapped contents by zwitterionic and cationic liposomes in ascites fluid at

37°C for 30 days.

Time [days]	Zwitterionic Liposomes	Cationic Liposomes
	$\Delta q \times 100$*	
1	0±9	0±12
2	0±9	-9±10
3	0±8	-4±11
10	19±8	1±10
15	21±7	0±9
20	47±7	26±9
30	69±7	52±9

* Fractional fluorescence self-quenching decrease due to calcein leakage from PEGylated

liposomes over time ($\Delta q_{day\_x}=(q_{day\_1}-q_{day\_x})/ q_{day\_1}$). After the first 15 days a maximum of

21% in self-quenching decrease was measured for all liposomes. The uncertainties
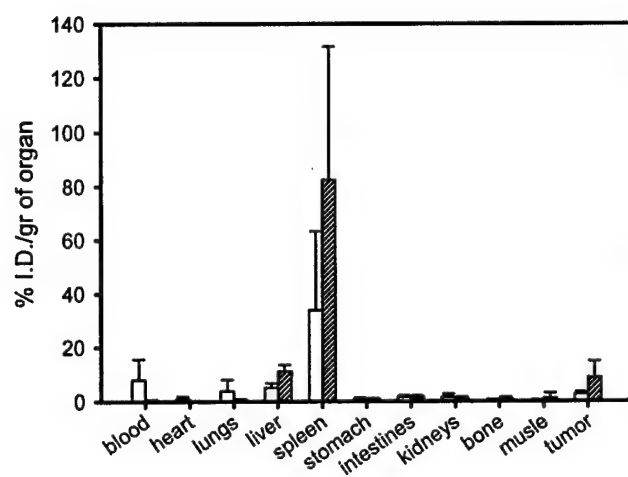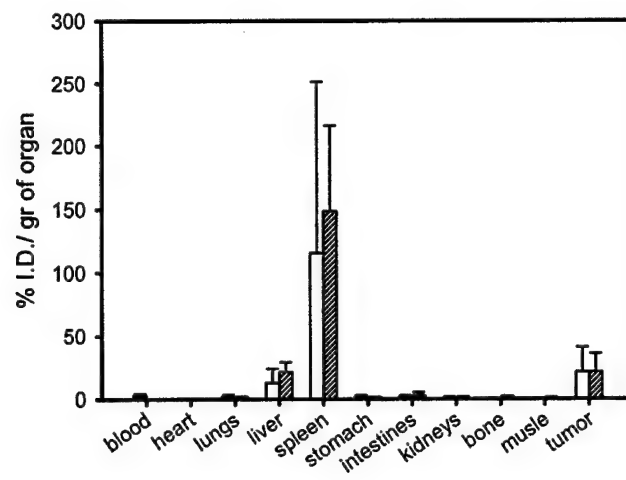
correspond to standard errors of repeated measurements.
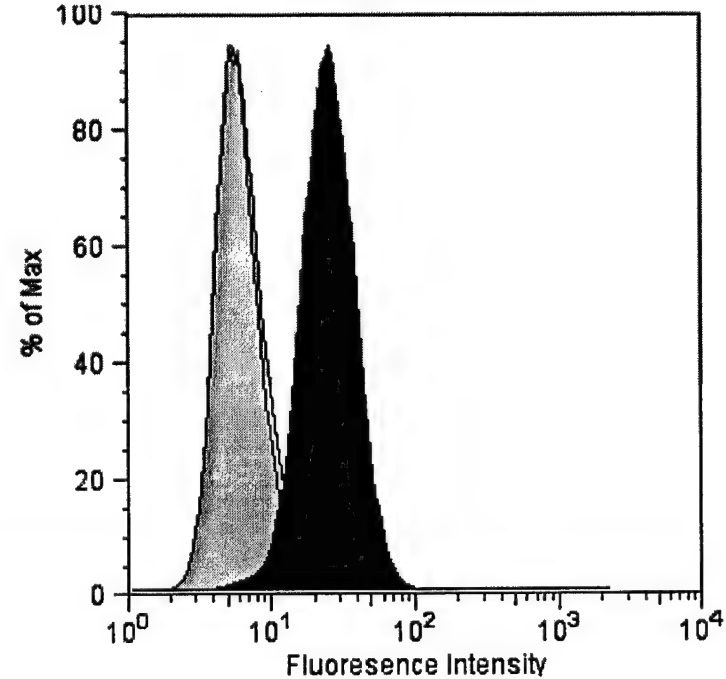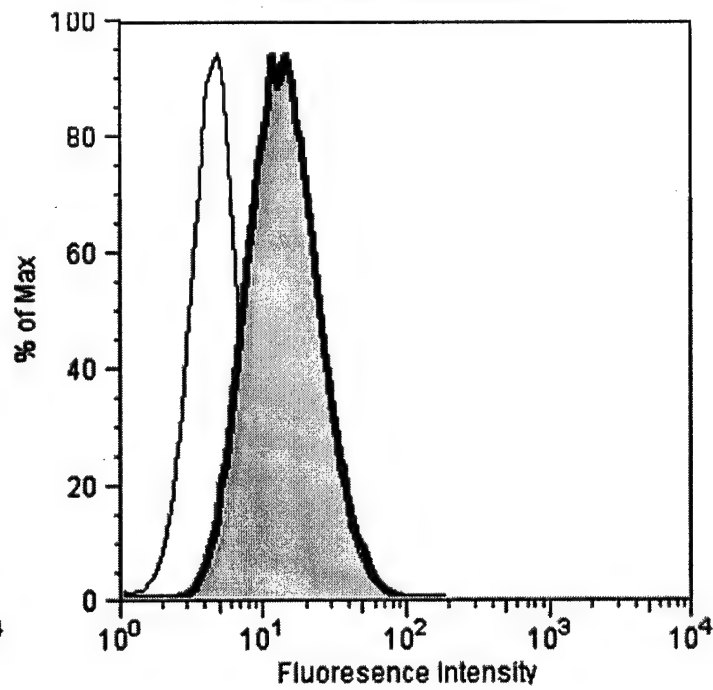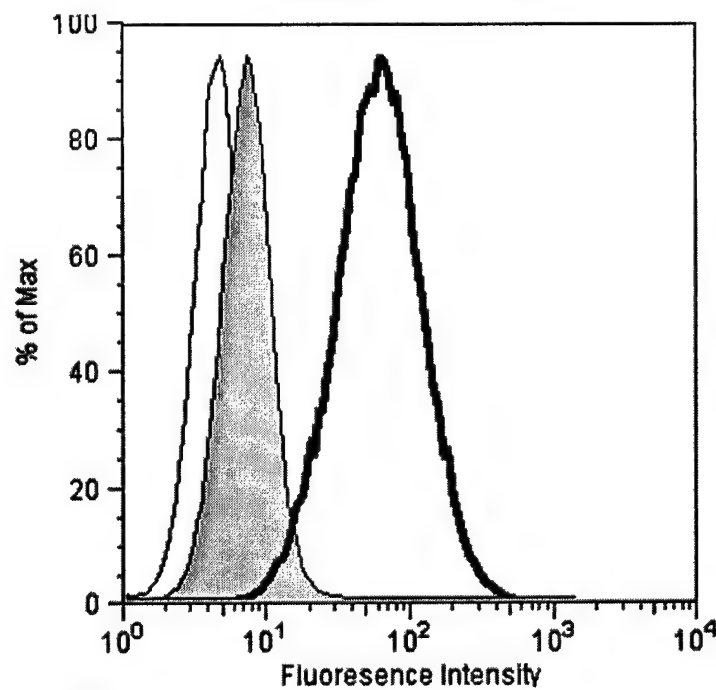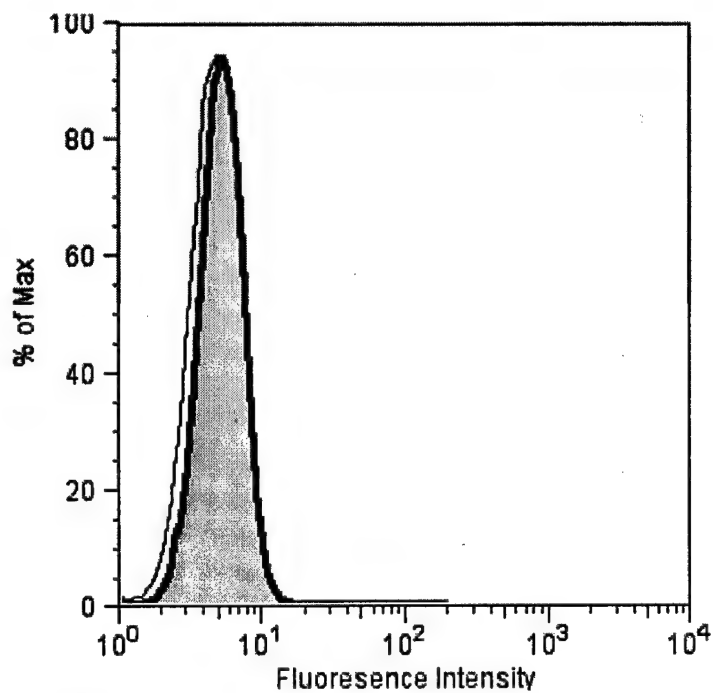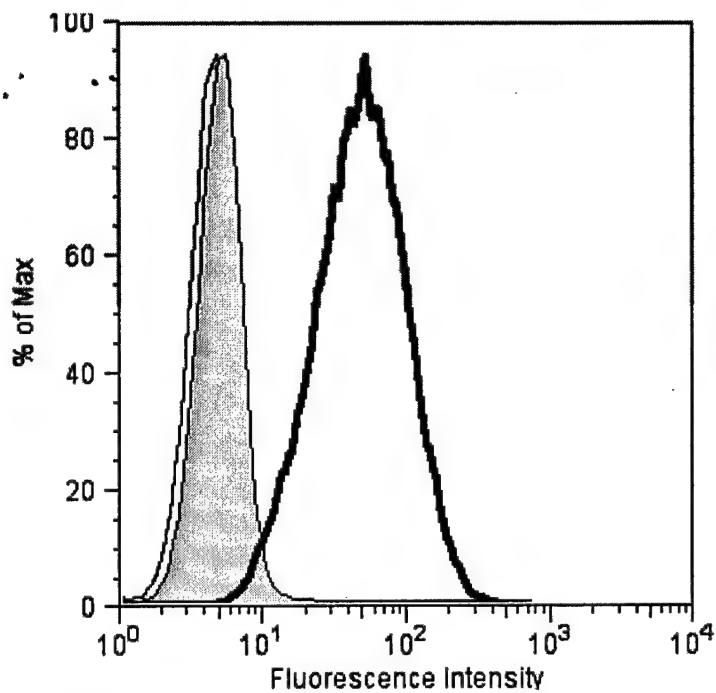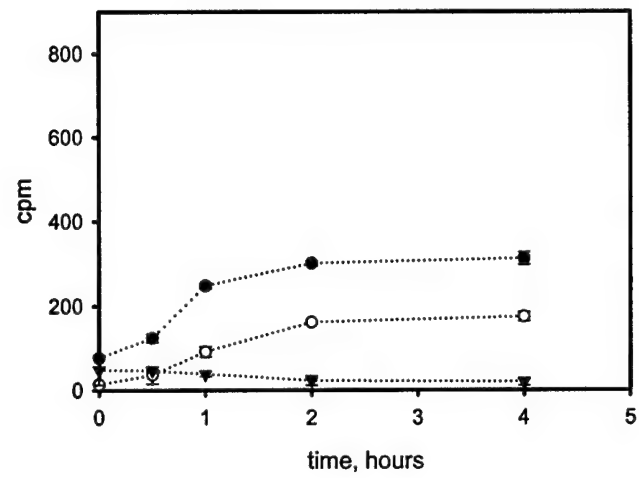
Figure 2A
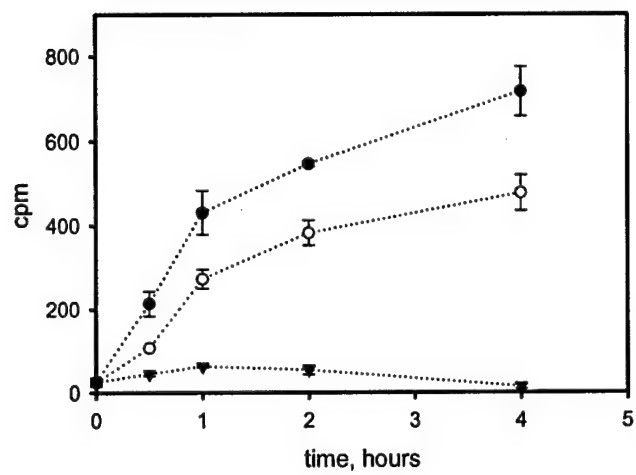
Figure 2B
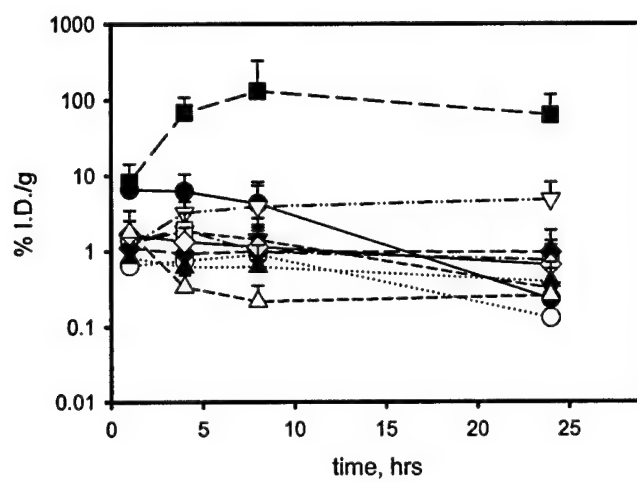
Figure 3A
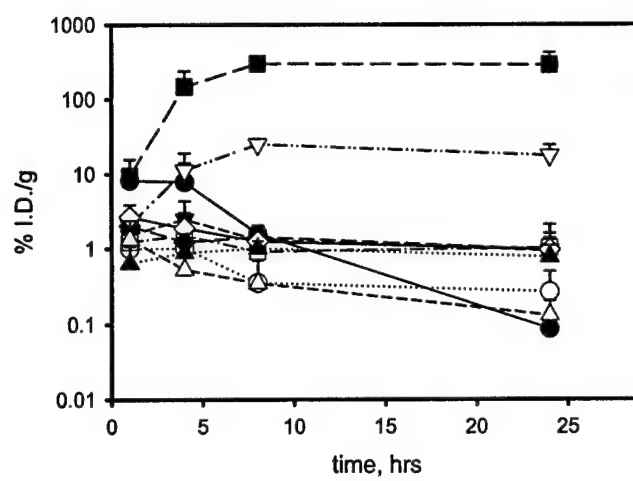
Figure 3B
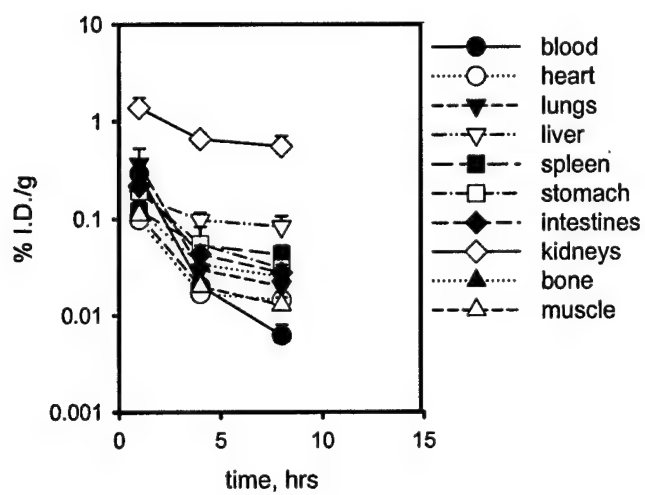
Figure 3C
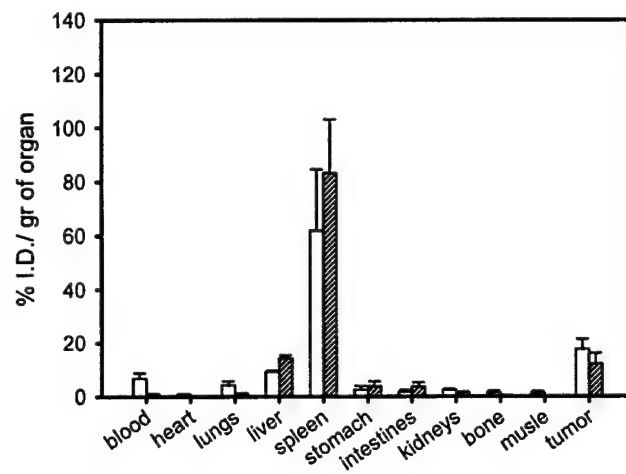
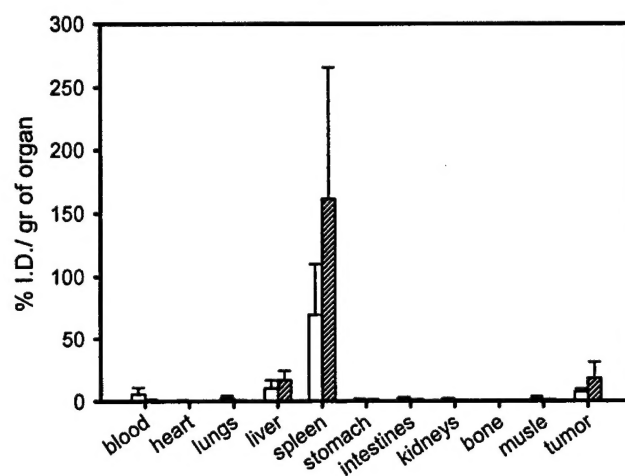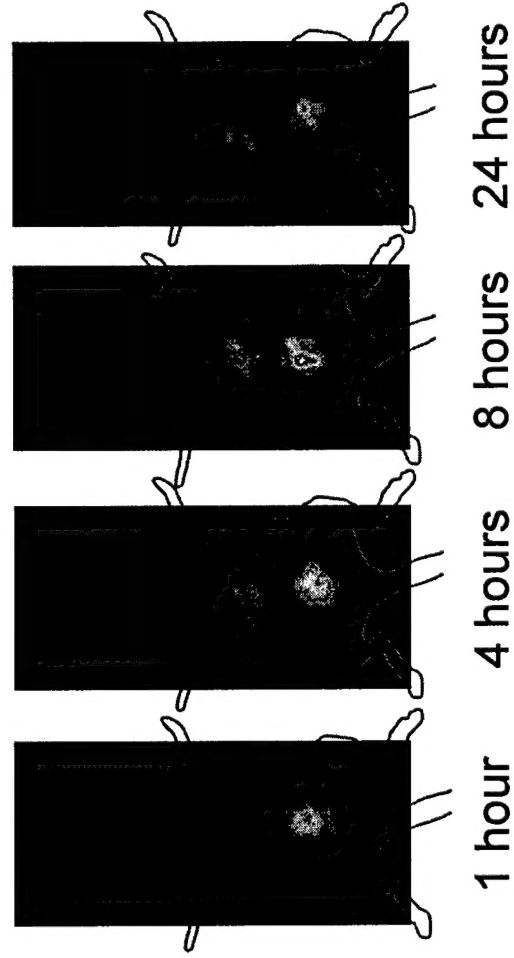Figure 4A

Figure 4B

Figure 5A

Figure 5B

1 hour   4 hours   8 hours   24 hours

Figure 6

Figure 7A

Figure 7B